Dynamical systems analysis of tachyon-dark-energy models from a new perspective

Saddam Hussain,[1,*] Saikat Chakraborty,[2,3,†] Nandan Roy,[4,‡] and Kaushik Bhattacharya[1,§]

[1]*Department of Physics, Indian Institute of Technology, Kanpur, Uttar Pradesh 208016, India*
[2]*The Institute for Fundamental Study "The Tah Poe Academia Institute", Naresuan University, Phitsanulok 65000, Thailand*
[3]*Center for Space Research, North-West University, Mahikeng 2745, South Africa*
[4]*Centre for Theoretical Physics and Natural Philosophy, Mahidol University, Nakhonsawan Campus, Phayuha Khiri, Nakhonsawan 60130, Thailand*

(Received 10 November 2022; accepted 14 February 2023; published 10 March 2023)

In this work, we present a new scheme to study the tachyon-dark-energy model using dynamical systems analysis by considering parametrization of the equation of state (EOS) of the dark energy. Both the canonical and phantom field dynamics are investigated. In our method, we do not require any explicit form of the tachyon potential. Instead of the potential, we start with an approximate form of the EOS of the tachyon field. This EOS is phenomenologically motivated and contains some dimensionless parameters. Using our method, we can construct the dynamical system which gives rise to the time evolution of the Universe. We have considered two different parametrizations of the EOS and studied the phase space dynamics in detail. Our analysis shows Taylor series parametrization of the EOS has serious cosmological limitations. We have also provided an example of how this method can be applied to coupled tachyon models with a specific form of interaction. Our proposal is generic in nature and can be applied to other scalar field dark energy models.

DOI: 10.1103/PhysRevD.107.063515

I. INTRODUCTION

The phenomenon of accelerated expansion of the Universe [1–5] is still an unsolved mystery, even two decades after its discovery. It is generally believed that there exists some mysterious component with negative pressure that is behind this accelerated expansion, and it happens to be the dominant (70%) component of the Universe. The cosmological constant (Λ) [6] with the constant equation of state (EOS) ($w_\lambda = -1$) is the simplest and most successful model of the accelerated expansion of the Universe. Because of its success, the ΛCDM model in which the cosmological constant Λ is considered as the candidate of the dark energy is given the status of the standard model of dark cosmology; CDM stands for cold dark matter. Although the ΛCDM model is very successful in fitting the observed data, it seems that our Universe is very highly fine-tuned to cause the cosmological constant to start dominating at a very specific time so that the Universe can evolve into the present Universe. This is one of the conceptual problems that the cosmological constant faces and is named as the cosmic coincidence problem. To explain the origin of the cosmological constant, another discrepancy arises between the theoretically predicted value of it and the observed value, which is of the order of hundreds of magnitude. Recently, with the increment of our ability to constrain the cosmological parameters with higher precision, the ΛCDM model also face challenges coming from cosmological observations. The most important challenge at this moment is the Hubble (H_0) tension. The early Universe observations like the cosmic microwave background (CMB) Planck Collaboration [7], baryon acoustic oscillation (BAO) [8,9], big bang nucleosynthesis [10], and Dark Energy Survey (DES) [11–13], which consider the cosmological constant as a component of the dark energy, estimated a value of the Hubble parameter to be $H_0 \sim (67.0\text{–}68.5)$ km/s/Mpc, which is lower than the observed value $H_0 = (74.03 \pm 1.42)$ km/s/Mpc, obtained by observing the local Universe using the distance ladder method from SH0ES [14] and H0LiCOW [15] Collaborations. The current discrepancy between these two types of datasets is of the order of 6σ. These difficulties with cosmological constants indicate clearly that there may be new physics involved in the late-time evolution of the Universe, and, consequently, an alternative to the cosmological constant should be investigated. In fact, there are

*msaddam@iitk.ac.in
†Corresponding author.
saikatnilch@gmail.com
‡Corresponding author.
nandan.roy@mahidol.ac.th
§kaushikb@iitk.ac.in

recent claims that solving the H_0 tension issue does indeed require new late-time physics [16–19].

Dynamical dark energy models in which the EOS of it varies with time have been proposed as alternatives to the cosmological constant. A wide variety of such dynamical dark energy models are abundant in the literature; a few of them are quintessence, k-essence, phantom, chaplygin gas, tachyon models, holographic DE models, and so on [20–29]. But there is no consensus on a particular model, as each model has its benefits and drawbacks.

The quintessence scalar field model is the most popular and well-studied dark energy model after the ΛCDM model. Recent observations have constrained the EOS of the dark energy to be less than minus one. This fact has challenged the quintessence model, as with a canonical scalar field an EOS lower than minus one cannot be achieved. There has been increasing interest in scalar field dark energy with a noncanonical kinetic term, as for these models the EOS can have values below minus one. The simplest one is the phantom scalar field, which has negative kinetic energy. In the most general form, these models are known as k-essence models [30], and tachyon [31] is a special case of it with Dirac-Born-Infeld (DBI) type of action [32]. The concept of the tachyon field is inspired by string theory, where it arises naturally as a decay mode of the D-branes [26,33,34]. Later, it has been applied to cosmology and has been extensively investigated as a candidate for dark energy [35–39]. Recently, it has been also reported that distinguishing the tachyon dynamics from a quintessence scalar field is difficult [40,41].

In this work, we have considered that the dark sector of the Universe consists of the tachyon scalar field and a perfect barotropic fluid where the tachyonic sector is solely responsible for producing late-time acceleration of the Universe. Mathematically, the dark energy sector is described by the DBI action. To make our analysis more general, we have considered both the canonical tachyon field and the phantom tachyon scalar field by introducing a switch parameter ϵ in the action. According to common practice, some particular form of the tachyon potential is considered to study the dynamics of the tachyon field. One of the difficulties with the conventional approach is related to the arbitrariness of the choice of the potential. A wide variety of potentials can give rise to the same dynamics [42,43], and as a result it is hard to distinguish the potential from observational results. In this work, we have followed a different approach. Instead of choosing any specific tachyon potential, we have chosen some approximate forms of the EOS of the tachyon field. These equations are time dependent and parametrized phenomenologically. As we know the primary dark energy component must have an equation of state with a value near -1 from observational inputs, we have assumed some workable forms of the EOS which in one case is a Taylor-series-like expansion of the EOS around the present time. In another case, we have assumed an EOS of the tachyon field which closely resembles the EOS of dark energy when the Hubble parameter becomes approximately constant. In this paper, we have worked with these two kinds of EOS for the tachyon field. Using these approximate forms of the EOS, we have successfully generated the dynamics of the late-time Universe. Although the exact form of the potential of the scalar field is not necessary in our case, using our method one can approximately predict the form of the scalar field potential. The method presented here can be applied to models in which the tachyon field is coupled to matter. However, it cannot be readily applied to the general form of coupling considered in Ref. [44]. Nonetheless, a very similar interaction form, $\mathbb{Q} = Q\rho_b\dot{\phi}H$, can be analyzed using this method. The method which we have used is a very general one and can be used in other models of dynamical dark energy.

The paper is presented as follows: In Sec. II, we discuss about the mathematical setup of the tachyon model and the construction of the autonomous system. Section III deals with dynamical systems analysis of the tachyon model with two different parametrizations of the EOS. This study includes both the quintessence and phantom field. Here, we also discuss some subtleties with our analysis. We extend our approach to a coupled tachyon model and study the dynamics in Sec. IV. In Sec. V, we summarize and conclude our method and findings.

II. DYNAMICS OF THE TACHYON FIELD

Let us consider a homogeneous and isotropic universe described by the Friedmann-Lemaître-Robertson-Walker metric

$$ds^2 = -dt^2 + a^2(t)d\mathbf{x}^2,$$

where $a(t)$ is the scale factor specifying the expansion of the Universe. The dark energy sector is constituted by the tachyon field described by the DBI type of action, which is given by

$$\mathcal{S} = -\int V(\phi)\sqrt{1+\epsilon\partial^\mu\phi\partial_\mu\phi}\sqrt{-g}d^4x, \tag{1}$$

where the parameter $\epsilon = \pm 1$. The plus sign is for the canonical tachyon field with positive kinetic energy, and the minus sign is for the phantom-type tachyon field which has negative kinetic energy. The total action of the system consists of the Einstein-Hilbert action for gravity and the action describing the behavior of a relativistic perfect fluid. In a homogeneous, isotropic, and spatially flat universe, evolution equations for the various dynamical variables can be written as

$$H^2 = \frac{\kappa^2}{3}\left(\rho_b + \frac{V}{\sqrt{1-\epsilon\dot{\phi}^2}}\right), \tag{2a}$$

$$\dot{H} = -\frac{\kappa^2}{2}\left((\gamma_b - 1)\rho_b + \frac{\epsilon\dot{\phi}^2 V}{\sqrt{1-\epsilon\dot{\phi}^2}}\right), \tag{2b}$$

$$\ddot{\phi} + 3H\dot{\phi}(1-\epsilon\dot{\phi}^2) + \epsilon\frac{V'}{V}(1-\epsilon\dot{\phi}^2) = 0, \tag{2c}$$

where $H = \frac{\dot{a}}{a}$ is the Hubble parameter, γ is the equation of state parameter of the background field, and $P_b = (\gamma_b - 1)\rho_b$. In the above equations, $\kappa^2 \equiv 8\pi G$, where G is the universal gravitational constant. The dot represents a derivative with respect to cosmological time t. For pressureless dust $\gamma_b = 1$, and for radiation $\gamma_b = 4/3$. Since we are interested in the late-time dynamics of the Universe, from now onward we will consider the matter and tachyon field as the major components of the Universe and neglect the contribution from radiation. Henceforth in this paper, we will always assume $\gamma_b = 1$. The pressure (P_ϕ) and density (ρ_ϕ) of the scalar field are given, respectively, by

$$P_\phi = -V(\phi)\sqrt{1-\epsilon\dot{\phi}^2}, \qquad \rho_\phi = \frac{V(\phi)}{\sqrt{1-\epsilon\dot{\phi}^2}}. \tag{3}$$

We will now cast the above equations as a set of constrained autonomous equations and then find out the nature of the critical points using dynamical systems analysis.

In order to do so, we consider the following set of transformations:

$$x = \dot{\phi}, \qquad y = \frac{\kappa\sqrt{V(\phi)}}{\sqrt{3}H}, \qquad \lambda = -\frac{V_{,\phi}}{\kappa V^{\frac{3}{2}}},$$
$$\Gamma = V\frac{V_{,\phi\phi}}{V_{,\phi}^2}, \qquad \sigma^2 = \frac{\kappa^2\rho_b}{3H^2}. \tag{4}$$

One must note that in the present case the scalar field has inverse mass dimension and the potential has dimension of mass raised to the fourth power. The subscript on a variable following a comma, such as $V_{,\phi}$, represents derivative of V with respect to ϕ. Two subscripts after the comma imply two derivatives. These variables were first introduced in Ref. [45], and later they were used in Refs. [40,46]. The constrained equation from the Friedmann equation [Eq. (2a)] can be expressed in terms of dynamical variables as

$$1 = \sigma^2 + \frac{y^2}{\sqrt{1-\epsilon x^2}}. \tag{5}$$

Using Eqs. (2b) and (2c), the dynamical equations can be written as follows:

$$x' = -(1-\epsilon x^2)(3x - \sqrt{3}\epsilon\lambda y), \tag{6a}$$

$$y' = \frac{y}{2}\left[-\sqrt{3}\lambda x y - 3\sqrt{1-\epsilon x^2}y^2 + 3\right], \tag{6b}$$

$$\lambda' = -\sqrt{3}\lambda^2 x y\left(\Gamma - \frac{3}{2}\right). \tag{6c}$$

In the above equations, the prime represents derivatives with respect to $N \equiv \ln(a)$. For cosmological parameters of the scalar field like density parameter of the scalar field Ω_ϕ, equation of state parameter w_ϕ, and deceleration parameter q, the effective sound speed $c_s^2 = P_{\phi,X}/\rho_{\phi,X}$ [47], where $X = -(1/2)g^{\mu\nu}\partial_\mu\phi\partial_\nu\phi$, can be written in terms of these new variables as

$$\Omega_\phi = \frac{y^2}{\sqrt{1-\epsilon x^2}}, \tag{7}$$

$$\gamma_\phi \equiv 1 + \frac{P_\phi}{\rho_\phi} = \epsilon\dot{\phi}^2 = \epsilon x^2, \tag{8}$$

$$q \equiv -1 - \frac{\dot{H}}{H^2} = -\left(1 - \frac{3}{2}\gamma_b\right) - \frac{3}{2}y^2\frac{\gamma_b - \epsilon x^2}{\sqrt{1-\epsilon x^2}}, \tag{9}$$

$$\omega_{\rm tot} \equiv -\frac{2\dot{H} + 3H^2}{3H^2} = \gamma_b - 1 - y^2\frac{\gamma_b - \epsilon x^2}{\sqrt{1-\epsilon x^2}}, \tag{10}$$

$$c_s^2 = 1 - \epsilon x^2. \tag{11}$$

The EOS of the scalar field is $\gamma_\phi = 1 + \omega_\phi$, where $\omega_\phi = P_\phi/\rho_\phi$. One can see from the set of autonomous equations in Eq. (6) that it is not closed unless one gives the information about the function Γ or the form of the potential $V(\phi)$. Generally, these equations can be closed in two different ways. One can consider a particular form of the potential and find out the corresponding Γ from its definition, or one can consider a particular form of Γ and integrate back to get the corresponding class of potentials. This is the conventional approach used to solve such a set of autonomous equations. The difficulty arising from such a scheme is related to the fact that most of the time it becomes very difficult to guess the form of the potential or Γ which will give rise to physically relevant behavior of the Universe. One can use various forms of potential and predict the evolution of the late Universe in various cases.

In the present paper, we will not proceed in the conventional line. We will use a more phenomenological method to solve the autonomous system. In our present work, we start with some particular parametrization for the scalar field EOS (ω_ϕ). Using our prior knowledge from the recent cosmological observations [7], we expect the EOS for the dark sector will be around -1 or some preassigned value ω_0 (close to -1). By considering a parametrization of the ω_ϕ,

one will be able to find an expression of λ in terms of x and y, using the first two equations in the set of autonomous equations given in Eq. (6). For internal consistency, we will use the form of λ as obtained in the third autonomous equation and solve it. This solution will produce a form of the unspecified Γ as a function of x and y. In our approach, all our ignorance about the functional form of the potential will be reflected in the functional form of Γ. As a result of this procedure, the dimension of the phase space of our system will reduce from 3D to 2D as the variable λ becomes redundant.

III. PARAMETRIZATION OF EQUATION OF STATE OF DARK ENERGY

In the following section, we discuss the phase space dynamics of the tachyon scalar field model. We will consider two kinds of parametrization for ω_ϕ; the choice of these two parametrizations have different phenomenological motivations and can give rise to interesting cosmological dynamics.

A. First parametrization

In the first parametrization, the EOS of the scalar field is considered as

$$\omega_\phi(N) = -1 + \omega_1 N, \tag{12}$$

where ω_1 is a constant and can be constrained from observations. As mentioned earlier, here $N = \log(a)$. The above-mentioned parametrization has been inspired from Ref. [48], where a more general form of it was considered: $\omega_\phi(a) = \omega_0 - \omega' \log(a)$. There, ω' is the derivative[1] of ω_ϕ with respect to the scale factor a, i.e., $\omega' = \frac{d\omega}{da}|_{a=1}$. The constraints on ω_0 and ω' came from SNIa + BAO + $H(z)$ data, and the constrained values were given as $-1.09 \leq \omega_0 \leq -0.66$ and $-1.21 \leq \omega' \leq 0.25$. The constraint on matter density was reported as $0.26 \leq \Omega_M \leq 0.32$. In our case, we have taken $\omega_0 = -1$ and $\omega_1 = -\omega'$. Using Eq. (8), we can now write γ_ϕ as

$$\gamma_\phi = 1 + \omega_\phi = \omega_1 N = \epsilon x^2. \tag{13a}$$

Taking a derivative of Eq. (13), with respect to N, and equating the value of x' to the x' expression in Eq. (6a), we can derive another constraint equation as follows:

$$-2\epsilon x(1 - \epsilon x^2)(3x - \sqrt{3}\epsilon\lambda y) = \omega_1. \tag{14}$$

This constraint equation can be solved for λ:

$$\lambda = \frac{\frac{\omega_1}{1-x^2\epsilon} + 6x^2\epsilon}{2\sqrt{3}xy}. \tag{15}$$

To make the system of autonomous equations consistent, the λ' equation in Eq. (6c) should also be satisfied by the derivative of λ given in Eq. (15) with respect to N. From the above-mentioned consistency condition, it is possible to express $\Gamma = f(x, y)$. To find the expression of Γ, see Appendix A. As result of this procedure, the dynamical system now has essentially two independent variables, x and y. The phase space has reduced from 3D to 2D.

One can now write down the effective autonomous equations in 2D. The new 2D autonomous system is given by

$$x' = \frac{\omega_1}{2\epsilon x}, \tag{16a}$$

$$y' = \frac{1}{2}y\left[-3y^2\sqrt{1-\epsilon x^2} + 3(1-\epsilon x^2) - \frac{\omega_1}{2(1-\epsilon x^2)}\right]. \tag{16b}$$

One can notice that the system is symmetric under $x \mapsto -x$ and $y \mapsto -y$. One must note that by definition $y \geq 0$ and, consequently, the symmetry $y \mapsto -y$ is practically superficial, although that transformation is a symmetry here. Next, we study the phase space behavior of the canonical and phantom tachyon field for the current parametrization.

1. Canonical tachyon ($\epsilon = +1$)

We first present the dynamical system analysis for the case of a canonical tachyon field, where $\epsilon = 1$. For this case, the phase space is compact because of the constraint in Eq. (5). As a result, we have

$$0 \leq x \leq 1, \qquad 0 \leq y \leq (1 - x^2)^{1/4}. \tag{17}$$

We have confined our attention to the first quadrant in the x–y plane due to the symmetry $x \mapsto -x$, $y \mapsto -y$. Here, y is always a positive semidefinite variable. It is interesting to note that the phase space is bounded by the curve

$$y = (1 - x^2)^{1/4}, \tag{18}$$

which is the locus of the points in the phase space that corresponds to an entirely scalar-field-dominated cosmology, except for the point $(x, y) = (1, 0)$. This is because $\sigma = 0$ at all the points on this curve except for $(x, y) = (1, 0)$, as can be checked from Eq. (5). On the other hand, the line $y = 0$ is the locus of the points in the phase space that corresponds to an entirely matter-dominated cosmology, except for the point $(x, y) = (1, 0)$. This is because $\sigma = 1$ at all the points on this curve except for $(x, y) = (1, 0)$.

[1]Here, the prime does not specify a derivative with respect to N.

We face a problem when we want to find the fixed points of the system. The autonomous system given in Eq. (16) diverges at $x = 0$, 1, and it seems like the only possible fixed point is at $(x \to \infty, y = 0)$, which is outside the range specified in Eq. (17). But this conclusion would be wrong, because, for an autonomous system of equations to qualify as a dynamical system, it needs to be at least first-order differentiable [49,50], which is clearly violated by the system (16) at $x = 0$, 1. Therefore, one should *not* naively use the system in Eq. (16) to find the fixed points. This makes the analysis of the phase space behavior of the above-mentioned system difficult.

In Ref. [51], it has been suggested that a redefinition of the time coordinate can alter the form of the autonomous system of equations to make it differentiable while keeping the phase space behavior intact. In the altered form, the critical points of the system may appear inside the constrained phase space. Any redefinition of time alters the way the scale factor evolves. In our analysis, we are not directly working with cosmic time; we are working with $N = \log(a)$. A redefinition of time will produce a new $\bar{N}$. We define $\bar{N}$ as

$$dN \to d\bar{N} = \frac{dN}{x(1-x^2)}. \tag{19}$$

Sticking to the first quadrant ($x \geq 0$, $y \geq 0$), we see that $(d\bar{N}/dN) > 0$, implying that $\bar{N}$ is always an increasing function of N and, thus, our time redefinition is workable. Henceforth, we will work with $\bar{N}$, and all the primes over x and y must be understood as derivatives of the respective variables with respect to $\bar{N}$.

After the redefinition of the time variable, the dynamical system reduces to the following form:

$$x' = \frac{\omega_1}{2}(1-x^2), \tag{20a}$$

$$y' = \frac{1}{2}xy\left[-3y^2(1-x^2)^{3/2} + 3(1-x^2)^2 - \frac{\omega_1}{2}\right]. \tag{20b}$$

We emphasize that the time redefinition in Eq. (19), and, consequently, the regularized dynamical system in Eq. (20), is valid only in the first quadrant. In a forthcoming subsection, we will explicitly show the method using which one may construct the dynamics in the second quadrant if one knows the dynamics in the first quadrant. Here, we analyze the system in the first quadrant. There is only one fixed point $(x, y) = (1, 0)$. Since this fixed point lies at the intersection of the curve specified in Eq. (18) and the line $y = 0$, we cannot definitively determine the cosmology corresponding to this fixed point.

The nature of the critical point is tabulated in Table I. This critical point is stable (unstable) for $\omega_1 > 0$ ($\omega_1 < 0$) and nonhyperbolic for the special case of $\omega_1 = 0$, i.e., cosmological constant. The cosmology corresponding to this critical point is dominated by the kinetic part of the scalar field, and near it the scale factor is evolving as $a(t) \sim t^{2/3}$.

TABLE I. The nature of one of the critical points for the first parametrization corresponding to $\epsilon = +1$. The cosmological evolution corresponding to the fixed point can be derived from the expression of the deceleration parameter in Eq. (9).

Points	(x, y)	Eigenvalues	Stability	Cosmology
P_1	(1, 0)	$\{-\omega_1, -\frac{\omega_1}{4}\}$	Stable for $\omega_1 > 0$ Unstable for $\omega_1 < 0$	$a(t) \sim t^{2/3}$

The nature of the phase space plots around the point $x = 1$, $y = 0$ is shown in Figs. 1(a) and 1(b). The plots clearly show the stability issue related to this fixed point. Corresponding to this redefined autonomous system, we see that Γ becomes -1 for this critical point, which shows that at the late-time phase Γ becomes constant.

2. Phantom tachyon ($\epsilon = -1$)

Here, we present the results related to the phantom tachyon. For this case, $\epsilon = -1$, and, as a consequence, one can see from Eq. (5) that the phase space is not compact. We first try to compactify the phase space, as in that case only can we exhaustively show phase space dynamics. In the following, we compactify the phase space using the following prescription:

$$X = \frac{x}{\sqrt{1+x^2}}, \qquad Y = \frac{y}{\sqrt{1+y^2}}. \tag{21}$$

In terms of X and Y, the Friedmann constraint in Eq. (5) becomes

$$1 = \sigma^2 + \sqrt{1-X^2}\,\frac{Y^2}{1-Y^2}. \tag{22}$$

The phase space in the (X, Y) coordinates is compact, because, from the constraint equation Eq. (22),

$$0 \leq X \leq 1, \qquad 0 \leq Y \leq \frac{1}{(1+\sqrt{1-X^2})^{1/2}}, \tag{23}$$

where, again, we have confined our attention to the first quadrant because of the symmetry $x \mapsto -x$, $y \mapsto -y$. Similar to the previous case, the phase space is bounded by the curve

$$Y = \frac{1}{(1+\sqrt{1-X^2})^{1/2}}, \tag{24}$$

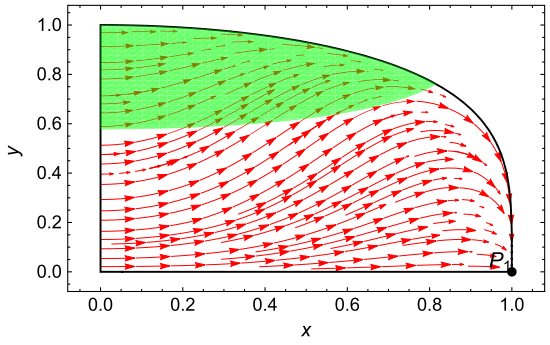

(a) The phase space plot for $\epsilon = +1, \omega_1 = 0.3$.

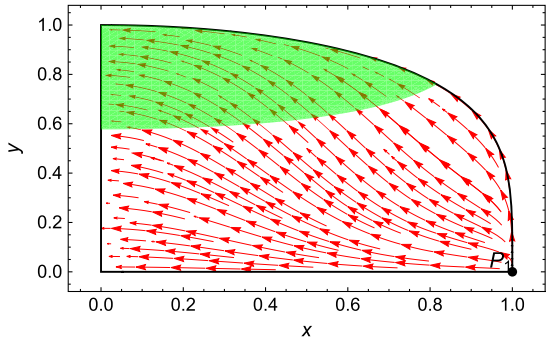

(b) The phase space plot for $\epsilon = +1, \omega_1 = -0.3$.

FIG. 1. The compact phase space for canonical tachyon with the parametrization given in Eq. (12). The phase space is compactified by the constraint Eq. (5). At the present epoch $N = 0$, $x = 0$ [see Eq. (13)]. The green region represents an accelerated phase with $-1 \leq \omega_{\rm tot} < -1/3$ [obtained using Eq. (10)]. The condition for the absence of gradient instability, namely, $0 \leq c_s^2 \leq 1$, is satisfied on the entire phase space.

which is the locus of the points in the phase space that corresponds to an entirely scalar-field-dominated cosmology, except for the point $(X, Y) = (1, 1)$. This is because $\sigma = 0$ at all the points on this curve except for $(X, Y) = (1, 1)$, as can be checked from Eq. (22). On the other hand, the lines $X = 1$ and $Y = 0$ are the locus of the points in the phase space that corresponds to an entirely matter-dominated cosmology, except for the point $(X, Y) = (1, 1)$. This is because $\sigma = 1$ at all the points on this line except for $(X, Y) = (1, 1)$.

The effective 2D autonomous dynamical system is described by the following equations:

$$X' = -\frac{\omega_1}{2X}(1 - X^2)^2, \tag{25a}$$

$$Y' = \frac{1}{2}Y\left[-\frac{3Y^2}{\sqrt{1 - X^2}} + \frac{3(1 - Y^2)}{1 - X^2} - \frac{\omega_1}{2}(1 - X^2)(1 - Y^2)\right]. \tag{25b}$$

Here, the primes designate differentiation with respect to $N = \log(a)$. From the above equations, it is seen that even after the compactification of the phase space the system diverges at $X = 0$, 1. To tackle this problem, we have adopted a similar strategy as adopted in the previous case. We redefine the time coordinate such that

$$dN \to d\bar{N} = \frac{dN}{X(1 - X^2)}. \tag{26}$$

Using $\bar{N}$, we can express the dynamical system in a new form as

$$X' = -\frac{\omega_1}{2}(1 - X^2)^3, \tag{27a}$$

$$Y' = \frac{1}{2}XY\left[-3Y^2\sqrt{1 - X^2} + 3(1 - Y^2) - \frac{\omega_1}{2}(1 - X^2)^2(1 - Y^2)\right], \tag{27b}$$

where the derivatives (primes) are now with respect to $\bar{N}$. We emphasize that the time redefinition in Eq. (26), and, consequently, the regularized dynamical system in Eq. (27), is valid only in the first quadrant. In the next subsection, we will explicitly show the method using which one may construct the dynamics in the second quadrant if one knows the dynamics in the first quadrant. Here, we present the dynamics of the system only in the first quadrant. There are two fixed points $(X, Y) = (1, 0), (1, 1)$ in the first quadrant. From the constraint in Eq. (22), it is clear that at the fixed point $(1, 0)$, $\sigma = 1$; i.e., the Universe near this fixed point is in a matter-dominated phase. The fixed point (1, 1) lies at the intersection of the curve specified in Eq. (24) and the line $X = 1$. Consequently, the cosmology corresponding to this fixed point cannot be determined definitively. The nature of the fixed points is tabulated in Table II. Note that the fixed points in this case are nonhyperbolic so that their stability cannot be inferred from a Jacobian analysis. Instead, their stability can be inferred investigating the nature of the various invariant submanifolds of the system. The mathematical analysis is presented in Appendix B. The phase space plots showing the nature of dynamical evolution around the fixed points are shown in Figs. 2(a) and 2(b). The two plots correspond to two values of ω_1; in one case $\omega_1 > 0$, and in the other case $\omega_1 < 0$.

3. Phase dynamics in the second quadrant

In the above discussion, we have focused our attention only to the first quadrant $x > 0$, $y > 0$, because the system

TABLE II. The nature of the critical point for first parametrization corresponds to $\epsilon = -1$.

Points	(X, Y)	Eigenvalues	Stability	Cosmology
P_1	(1, 0)	$(0, 3/2)$	Unstable for $\omega_1 > 0$ Saddle for $\omega_1 < 0$	Matter dominated
P_2	(1, 1)	$(0, -3)$	Saddle for $\omega_1 > 0$ Stable for $\omega_1 < 0$	Indeterminate

in Eq. (16) possesses the symmetry $x \mapsto -x$ and $y \mapsto -y$. The time redefinitions in Eqs. (19) and (26) and the regularized dynamical systems in Eqs. (20) and (27) are valid in the first quadrant only. Consequently, Figs. 1(a), 1(b), 2(a), and 2(b) all show the phase space dynamics in the first quadrant. As we argued before, the symmetry $y \mapsto -y$ is practically superficial, because by definition $y \geq 0$. One may, however, ask what would be the phase space dynamics in the second quadrant $x < 0$, $y > 0$. All possible cosmological scenarios with $\dot{\phi} < 0$ constitute the second quadrant. If we focus our attention to the second quadrant, the time redefinitions in Eqs. (19) and (26) should be modified as

$$dN \to d\bar{N} = \frac{dN}{-x(1-x^2)} \tag{28}$$

and

$$dN \to d\bar{N} = \frac{dN}{-X(1-X^2)}, \tag{29}$$

respectively. This is because one needs to respect the condition $(d\bar{N}/dN) > 0$ to preserve the arrow of time. The regularized dynamical systems in Eqs. (20) and (27) would then be modified only by an overall minus sign in front. Consequently, the phase space dynamics in the second quadrant will just be a reflection of that in the first quadrant against the line $x = 0$ or $X = 0$.

In fact, this can be also argued as follows. The dynamical system in Eq. (16) is of the form

$$u_x = f_x(x, y), \qquad u_y = f_y(x, y), \tag{30}$$

where $u_{x,y}$ are the Cartesian components of the "phase flow" at each point (x, y). The functions $f_{x,y}(x, y)$ are such that $f_x(-x, y) = -f_x(x, y)$ and $f_y(-x, y) = f_y(x, y)$. As one goes from first to second coordinate, the x component of the flow velocity is inverted, whereas the y component remains intact. As a result of these observations, we see the phase space dynamics in the first quadrant is given by Fig. 1(a) or 1(b) for the canonical tachyon and Fig. 2(a) or 2(b) for the phantom tachyon. The phase space dynamics in the second quadrant will be a reflection of these plots against $x = 0$.

We also notice that the first and second quadrants are completely disjoint. There is no direct way to "glue" the phase portraits of the first quadrant with corresponding portraits in the second quadrant. This is related to the time redefinitions we have used, and, consequently, the regularized dynamical systems are valid in only either the first quadrant or the second quadrant. The physical interpretation of this fact is that the time derivative of the field, $\dot{\phi}$, cannot change sign at any point during the cosmic evolution. One can also interpret this in another way.

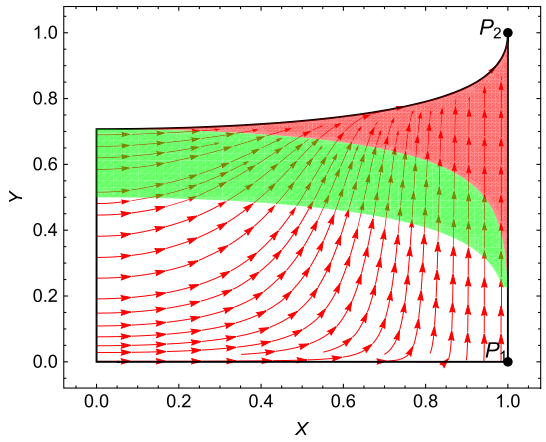

(a) The phase space plot for $\epsilon = -1, \omega_1 = -0.5$.

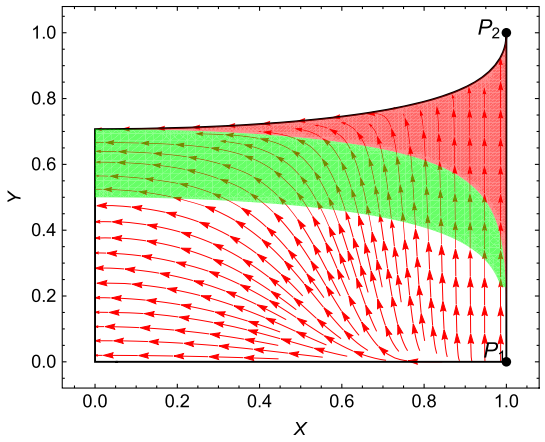

(b) The phase space plot for $\epsilon = -1, \omega_1 = 0.5$.

FIG. 2. The compact phase space for a phantom tachyon with the parametrization given in Eq. (12). The phase space is compactified by the constraint Eq. (22). At the present epoch $N = 0$, $x = 0$. The green region represents an accelerated phase with $-1 \leq \omega_{\text{tot}} < -1/3$. The red region represents the phantom phase with $\omega_{\text{tol}} < -1$.

Note that the nature of the fixed points remains the same irrespective of whether one considers the first quadrant or the second quadrant. As a result, one may conclude that the actual sign of $\dot{\phi}$ does not really matter as the cosmological dynamics is concerned. Whether it is positive or negative, the cosmological dynamics remains the same.

4. Analytical solution for the asymptotic behavior

For the particular parametrization that we have considered here, it is possible to analytically confirm the results that we have found from the phase space analysis. The parametrization essentially fixes the solution for $x(N)$ from Eq. (13):

$$\epsilon x^2(N) = \omega_1 N. \tag{31}$$

The equation for $y(N)$ is then

$$\frac{dy(N)}{dN} = \frac{1}{2}y\left[-3y^2\sqrt{1-\omega_1 N} + 3(1-\omega_1 N) - \frac{\omega_1}{2(1-\omega_1 N)}\right]. \tag{32}$$

Let us now find out the asymptotic behavior for canonical and phantom tachyons.

(i) *For canonical tachyon* ($\epsilon = 1$) *and* $x^2(N) = \omega_1 N$.—For $\omega_1 > 0$, the solution is well defined in the future up to a finite e-folding $N = N_{\rm max} = 1/\omega_1$ but undefined in the past. For $\omega_1 < 0$, the solution is well defined in the past up to a finite e-folding $N = N_{\rm min} = 1/\omega_1$ but undefined in the future. The finite value $N_{\rm max,min}$ comes from demanding $1 - \omega_1 N > 0$, which is required for $\frac{dy(N)}{dN}$ to be real. We emphasize that a finite value for the e-folding N corresponds to a finite value of the scale factor $a(t)$ but does *not* necessarily correspond to a finite value of the cosmological time t. As $N \to N_{\rm max,min}$, $x \to 1$ and

$$\frac{dy(N)}{dN} \sim \frac{y}{4(N - \frac{1}{\omega_1})}. \tag{33}$$

Integrating the above, we get

$$y(N) \sim \left|N - \frac{1}{\omega_1}\right|. \tag{34}$$

Therefore, $y(N) \to 0$ as $N \to N_{\rm max,min}$. This is consistent with the results obtained in Sec. III A 1, as the fixed point P_1, which is a future attractor for $\omega_1 > 0$ and a past attractor for $\omega_1 < 0$, has the coordinates $(x, y) = (1, 0)$.

(ii) *For a phantom tachyon* ($\epsilon = -1$) *and* $x^2(N) = -\omega_1 N$.—For $\omega_1 > 0$, the solution is well defined in the past but undefined in the future. For $\omega_1 < 0$, the solution is well defined in the future but undefined in the past. As $N \to \pm\infty$, $x \to \infty$ ($X \to 1$) and

$$\frac{dy(N)}{dN} \sim -\frac{3}{2}y\omega_1 N. \tag{35}$$

Integrating the above, we get

$$y(N) \sim e^{-\frac{3}{4}\omega_1 N^2}. \tag{36}$$

Therefore, $y(N) \to 0$ ($Y \to 0$) as $N \to -\infty$ for $\omega_1 > 0$ and $y(N) \to \infty$ ($Y \to 1$) as $N \to \infty$ for $\omega_1 < 0$. This is consistent with the results obtained in Sec. III A 2, as the fixed point $P_1 \equiv (X, Y) = (1, 0)$ is a past attractor for $\omega_1 > 0$ and $P_2 \equiv (X, Y) = (1, 1)$ is a future attractor for $\omega_1 < 0$.

5. Some comments about Taylor series approximation

The parametrization that we have worked with in this section, namely, the one given by Eq. (12), is the first-order Taylor series approximation of $\omega_\phi(N)$ around the present epoch $N = 0$. The coefficients of the Taylor expansion can be constrained via observations. As a first approximation, we have assumed that the first-order Taylor series approximation of $\omega_\phi(N)$ remains valid for the entire domain of consideration. One can take into account higher-order terms in the Taylor series to get a better approximation for $\omega_\phi(N)$. Nonetheless, our analysis with the first-order Taylor series approximation suffices to establish the generic methodology to work with Taylor series parametrizations. For example, consider the parametrization containing the second-order Taylor series approximation

$$\omega_\phi = -1 + \omega_1 N + \omega_2 N^2, \tag{37}$$

which gives

$$\epsilon x^2 = \omega_1 N + \omega_2 N^2. \tag{38}$$

For the first-order Taylor series parametrization in Eq. (12), we have taken the derivative of Eq. (13) once with respect to N and then used the dynamical equation of x from Eq. (6) to arrive at the constraint in Eq. (14). For the second-order Taylor series parametrization given in Eq. (37), we need to take the derivative of Eq. (13) twice with respect to N and use the dynamical equations in Eq. (6) in place of x', y', and λ' to arrive at a similar constraint equation. In general, if one takes the nth-order Taylor series approximation as the parametrization for $\omega_\phi(N)$, one needs to take derivatives with respect to N, n times, and use the dynamical equations in Eq. (6) at each step to replace of x', y', and λ'.

Although the Taylor series parametrization has a straightforward motivation, there is a serious drawback with this parametrization as long as tachyonic dark energy

is concerned. As we have seen with the first-order Taylor series parametrization in Sec. III A 4, the solution $x(N)$ is undefined in either the past ($N < 0$) or future ($N > 0$). This is not a unique result valid only for the first-order parametrization. Even for higher-order Taylor series parametrizations, the solution will always be undefined in either the past or future. As a consequence of this, the Taylor series parametrizations of any order can be used to describe the cosmological dynamics either from the matter-dominated epoch in the past up to the present epoch or from the present epoch up to some future asymptotic time but *not* an entire dynamics starting from the matter-dominated epoch in the past through the present day to a future asymptotic. One can infer that Taylor series parametrizations are not really compatible with tachyonic-dark-energy models.

B. Second parametrization

The issues with the Taylor series parametrizations that we have pointed out in Sec. III A 5 motivate us to try other parametrizations for the equations of state of tachyonic dark energy. Here, we consider the parametrization studied in Refs. [52,53]. This is a completely different way of parametrizing a time-dependent EOS of the scalar field. The parametrization is given as

$$\omega_\phi = \omega_0 + \omega_1(t\dot{H}/H). \tag{39}$$

In this parametrization, ω_0 and ω_1 are dimensionless constant parameters. In this parametrization, $\omega_\phi \to \omega_0$ in a pure dark-energy-dominated phase, where $\dot{H} \sim 0$. The factor t/H is included before $\dot{H}$ to make ω_1 dimensionless. This parametrization can be associated with the field equations via the equation of state $\omega_\phi = -1 + \epsilon x^2$. The last equation can also be written as $1 + \omega_0 + \omega_1(t\dot{H}/H) = \epsilon x^2$. Taking the derivative of this equation with respect to t and then converting the derivatives in terms of N, for the case where $\omega = 0$, one gets a relation as

$$\begin{aligned} x' = {} & \frac{1}{2\epsilon - (\epsilon x^2 - 1 - \omega_0)(2/x^2 + \epsilon/(1-\epsilon x^2))} \\ & \times \left[\frac{3}{2}\frac{\epsilon x y^2}{\sqrt{1-\epsilon x^2}}(-\omega_1 + \epsilon x^2 - 1 - \omega_0)\right. \\ & \left. - \sqrt{3}\lambda y(\epsilon x^2 - 1 - \omega_0)\right]. \end{aligned} \tag{40}$$

Equating this expression of x to the value of x' in Eq. (6), one can find out a constraint for the variable λ as

$$\lambda = \frac{\frac{3xy^2\epsilon(x^2\epsilon-\omega_0-\omega_1-1)}{2\sqrt{1-x^2\epsilon}\left[2\epsilon-\left(\frac{\epsilon}{1-x^2\epsilon}+\frac{2}{x^2}\right)(x^2\epsilon-\omega_0-1)\right]} - 3x(x^2\epsilon-1)}{\frac{\sqrt{3}y(x^2\epsilon-\omega_0-1)}{2\epsilon-\left(\frac{\epsilon}{1-x^2\epsilon}+\frac{2}{x^2}\right)(x^2\epsilon-\omega_0-1)} - \sqrt{3}y\epsilon(x^2\epsilon-1)}. \tag{41}$$

In this dynamical system, λ is related to the derivative of the potentials. In our approach, we are not working with the exact form of the scalar field potential; we are using an extra condition consistently, which reduces the phase space dimension by one. If we take the derivative of this λ in Eq. (41) with respect to N and equate the resultant expression with the one appearing in Eq. (6c), we will get the form of Γ in terms of x and y. One can find the evolution of Γ in terms of x and y. In this way, Eq. (41) provides another constraint on the system which reduces the phase space dimension from 3D to 2D.

1. Canonical tachyon ($\epsilon = +1$)

For the normal tachyon field, the expression of λ from Eq. (41) becomes

$$\lambda = -\frac{\sqrt{3}(-4\sqrt{1-x^2}x(\omega_0+1) + x^5(2\sqrt{1-x^2}-y^2) + x^3(2\sqrt{1-x^2}(\omega_0+1) + y^2(\omega_0+\omega_1+1)))}{4(1-x^2)^{3/2}y(\omega_0+1)}. \tag{42}$$

Here, we can see that λ becomes singular at $x = \pm 1$, $y = 0$, and $\omega_0 = -1$. Differentiating λ with respect to N gives

$$\begin{aligned} \lambda' = {} & \frac{1}{4(1-x^2)^{5/2}y^2(\omega_0+1)}\sqrt{3}\left[2x(1-x^2)^{3/2}(x^4 + x^2(\omega_0+1) - 2(\omega_0+1))y'\right. \\ & + x^3(x^2-1)y^2y'(-x^2+\omega_0+\omega_1+1) - x^2y^3x'(2x^4 - 5x^2 + 3(\omega_0+\omega_1+1)) \\ & \left. + 2\sqrt{1-x^2}y(3x^6 + x^4(\omega_0-4) - x^2(\omega_0+1) + 2(\omega_0+1))x'\right]. \end{aligned} \tag{43}$$

Equating the above equation with Eq. (6c) produces the expression of Γ. The expression of Γ is presented in Appendix C.

Using the above techniques, the phase space dimension reduces by one, and the autonomous equations of the effective system can be expressed as

$$x' = -\frac{3x^3[x^2(2\sqrt{1-x^2}-y^2) - 2\sqrt{1-x^2}(\omega_0+1) + y^2(\omega_0+\omega_1+1)]}{4\sqrt{1-x^2}(\omega_0+1)}, \tag{44a}$$

$$y' = \frac{1}{2}y\left[-3\sqrt{1-x^2}y^2 + \frac{1}{4(1-x^2)^{3/2}(\omega_0+1)}3x\left(-4\sqrt{1-x^2}x(\omega_0+1) + x^5(2\sqrt{1-x^2}-y^2) + x^3\left(2\sqrt{1-x^2}(\omega_0+1) + y^2(\omega_0+\omega_1+1)\right)\right)\right]. \tag{44b}$$

Although y is by definition defined only in the positive branch—i.e., it is always positive in our case (with zero minimum)—we see that the above set of equations has the symmetry $x \mapsto -x$ and $y \mapsto -y$. This symmetry is reflected in the table of fixed points. We tabulate all the fixed points of the system, although physically only the positive values of y are significant. We have found the fixed points of the above set of autonomous equations, and these critical points are tabulated in Table III. In the present case, there are eight critical points which are dependent on the values of ω_0 and ω_1. To find the stability of each point, we linearize the autonomous system around the fixed point and find the Jacobian matrix. The eigenvalues of the Jacobian matrix are E_1 and E_2. Based on the sign of the real coefficients of the eigenvalues, the stability of the system is determined. The eigenvalues of the system have been tabulated in Table III. A fixed point is stable (unstable) if all the eigenvalues have real negative (positive) parts. For alternate signs of the real parts of eigenvalues, the point becomes a saddle point. If any eigenvalue becomes zero for a fixed point, then the system's stability will no longer be determined by linearization. In the last case, one can either employ the center manifold theorem or find it numerically by solving the differential equation. In order to understand the nature of the points, the total EOS, $\omega_{\rm tot}$, and sound speed, c_s^2, of the system have been shown in Table IV.

Out of the eight critical points, two critical points are only ω_0 dependent, and these are denoted by $P_{1,2}$. These critical points exists for $\omega_0 \geq -1$. The eigenvalues for these points show that they are saddle points for $-1 < \omega_0 < 0$ and stable points for $\omega_0 > 0$. These points share $\omega_{\rm tot} = 0$, which signifies the matter phase of the Universe. From the sound speed limit $0 \leq c_s^2 \leq 1$, we infer that ω_0 must take negative values.

There is a set of critical points, consisting of points $P_{7,8}$, where the points are constants. For this set, one of the eigenvalues becomes zero, for each element, and, hence, the stability of the points cannot be determined in a conventional way. To find the stability of these critical points, we used the numerical technique and found that the points are stable. The EOS and sound speed around these points are -1 and 1, respectively.

TABLE III. The critical points in the second parametrization.

Critical points for $\epsilon = +1$			
Points	x	y	Eigenvalues (E_1 and E_2)
P_0	0	0	$(0, 3/2)$
$P_{1,2}$	$\mp\sqrt{1+\omega_0}$	0	$-3(1+\omega_0), -3\omega_0/2$
$P_{3,4}$	$-\sqrt{1+\omega_0-\omega_1}$	$\mp(-\omega_0+\omega_1)^{1/4}$	$\frac{-3}{2(1+\omega_0)}(1+\omega_0-\omega_1)^2,\ 3(\omega_0-\omega_1)$
$P_{5,6}$	$\sqrt{1+\omega_0-\omega_1}$	$\mp(-\omega_0+\omega_1)^{1/4}$	The same as above
$P_{7,8}$	0	∓ 1	$(-3, 0)$

TABLE IV. The critical points and their nature for $\epsilon = 1$, corresponding to $\omega_0 = -0.9$ and $\omega_1 = -0.05$.

Points	(x, y)	$\omega_{\rm tot}$	c_s^2	Γ	λ	Stability
P_0	(0, 0)	0	1	∞	∞	Unstable
$P_{1,2}$	$(\mp 0.32, 0)$	0	$-\omega_0$	$\frac{1}{2\omega_0+2}+1$	∞	Saddle
$P_{3,4}$	$(-0.39, \mp 0.96)$	$\omega_0-\omega_1$	$-\omega_0+\omega_1$	3/2	$\pm\frac{\sqrt{3}\sqrt{\omega_0-\omega_1+1}}{\sqrt[4]{\omega_1-\omega_0}}$	Stable
$P_{5,6}$	$(0.39, \mp 0.96)$	$\omega_0-\omega_1$	$-\omega_0+\omega_1$	3/2	$\mp\frac{\sqrt{3}\sqrt{\omega_0-\omega_1+1}}{\sqrt[4]{\omega_1-\omega_0}}$	Stable
$P_{7,8}$	$(0, \pm 1)$	-1	1	∞	0	Stable

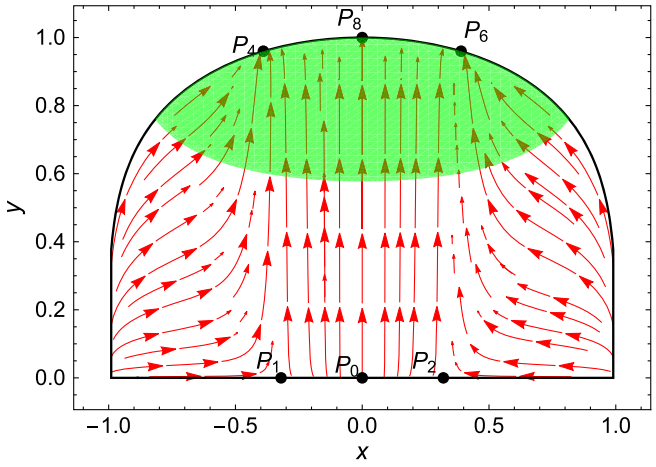

FIG. 3. The phase space plot for $\epsilon = 1$, $\omega_0 = -0.9$, and $\omega_1 = -0.05$. The phase space is constrained from Eq. (2a). In the green region, $-1 \leq \omega_{\rm tot} < -1/3$.

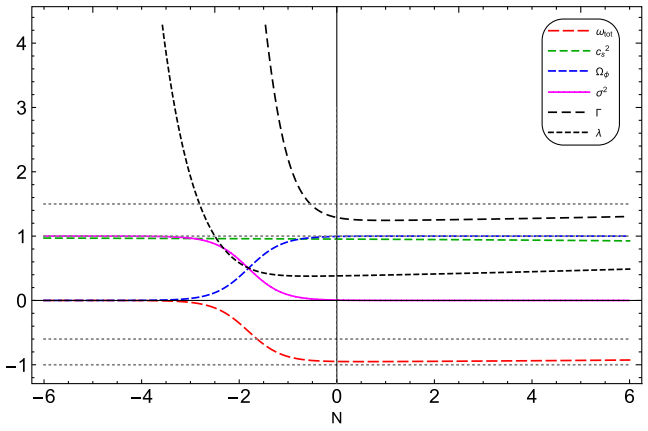

FIG. 4. The evolution plot for $\epsilon = 1$, $\omega_0 = -0.9$, and $\omega_1 = -0.05$.

The rest of the critical points from P_3 to P_6 are ω_0 and ω_1 dependent. In order to have real critical points, $(\omega_0 - \omega_1) \geq -1$. For stable fixed points, one requires $\omega_0 < \omega_1$. In order to produce the accelerating solution, we require $\omega_{\rm tot} < -1/3$, and from the sound speed condition we find that $\omega_{\rm tot} = -c_s^2$. From this, we observe that, as $\omega_{\rm tot}$ approaches -1, sound speed becomes 1. Hence, we may infer that by taking negative values of ω_0 and ω_1 one may obtain the desired late-time dynamics of the Universe. Hence, for further analysis we have chosen $\omega_0 = -0.9$ and $\omega_1 = -0.05$.

The phase portrait of the system has been shown in Fig. 3. There are two separate regions in the phase plot. The green regions represent the accelerated expansion phase of the Universe, whereas the white region represents the decelerated expansion phase of the Universe. One can clearly see all the solutions for the considered values of $\omega_0 = -0.9$ and $\omega_1 = -0.05$ specifying the decelerated expansion phase are on the $y = 0$ line. This implies that deep in the matter-dominated era the potential of the scalar field was close to zero, and after that the potential becomes nontrivial, giving rise to the dynamics of the scalar field. The phase space is symmetric around both the x and y axes. We have plotted only the physically significant region. The sound speed limit remains between 0 and 1 in the entire region. The trajectories are attracted toward P_4, P_6, and P_8. All these points are scalar-field-dominated fixed points. From Table IV, these fixed points are stable in nature and act as late-time attractors.

We have plotted the system variables such as $\omega_{\rm tot}$, c_s^2, Ω_ϕ, σ^2, Γ, and λ in Fig. 4 with respect to N by solving the autonomous equations for x' and y'. In the early epoch of the Universe, the EOS of the system starts from 0 when the fluid energy density parameter σ^2 dominates over the scalar field energy density parameter. At this epoch, the sound speed is nearly 1, and both λ and Γ are significantly large. As the Universe evolves, the EOS decreases toward the negative value, and, at some point where the tachyon field energy density has increased significantly, the EOS becomes saturated to -0.85. In the last phase, the parameter λ saturates at <1.3, whereas Γ saturates at 0.4. The system's late-time EOS can go very close to -1 depending on the choice of ω_0 and ω_1. This signifies that the nonphantom tachyon field can describe the late-time acceleration with significant sound speed.

Although in our formalism one does not need the exact form of the potential, as the form of the EOS of the scalar field modifies the autonomous equations and produces the desired dynamics of the system, one may approximately find out the form of the potential using the phase space dynamics. Here, we present an approximate scheme using which the form of $V(\phi)$ can be found out. The method discussed here is a general one and can be applied to most of the cases discussed in this paper. Because the functional form of the potential is not required in our case, we have not calculated the potential in all other cases. If one is really interested to know the approximate form of the potential, then the method discussed below can always be used. To find out the functional form of the potential, we will use the definition $\lambda = -\frac{V_{,\phi}}{\kappa V^{3/2}}$. In the present case, λ is a function of x and y as given in Eq. (41). From the autonomous equation, we have found the evolution of x and y in terms of $N = \log a$. We can express $V(\phi)$ in terms of dynamical variables as

$$\kappa \int \lambda {\rm d}\phi = -\int \frac{{\rm d}V}{V^{3/2}},$$

which yields

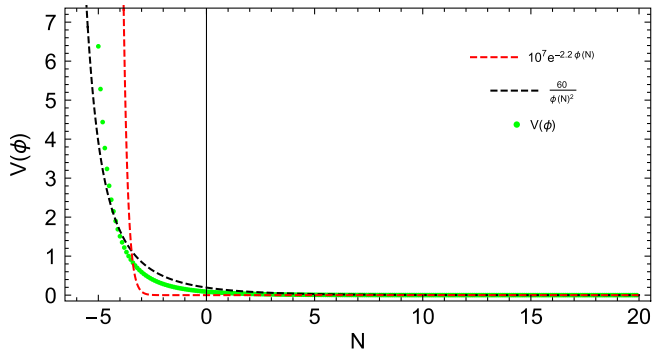

FIG. 5. The exact potential and its approximations for $\epsilon = 1$, $\omega_0 = -0.9$, and $\omega_1 = -0.05$.

$$\left[\kappa/2 \int \lambda \frac{x}{H} \mathrm{d}(\log a)\right]^{-2} = V(\phi). \tag{45}$$

In the above equation, H can be expressed in terms of the phase space variables x and y.[2] We can then numerically integrate and find the form of the potential of the system, expressed as a function of N. In Fig. 5, we have found the potential $V(\phi)$, which is evolving with $\log a$, by assuming $\kappa = 1$. The exact form of the potential obtained from this process is shown in green. We see that at the early epoch the potential of the tachyon field is relatively very high, and as the system evolves the potential saturates at a lower value. The potential becomes considerably low at the late-time phase of the Universe. One can approximately find the functional form of the potential. Here, we present two possible forms. It is seen that $V(\phi) = 60/\phi^2$ nicely fits the actual green curve.[3] This kind of a potential often arises in k-essence models. There is another possible form of the potential given by $V(\phi) = 10^7 \times e^{-2.2\phi}$. This form of the potential also closely matches with the exact value of $V(\phi)$ in the late phase of the Universe, whereas in the very early phase this approximation does not work. This form of potential is generally used in quintessence models. These two forms of the approximate potential show that our analysis can predict a functional form of $V(\phi)$ if required. Henceforth, we will not calculate the functional form of $V(\phi)$, as this form is not required to predict the dynamics of our system.

[2]In this regard, one must note that one can also use the definition of $\Gamma(N)$ to determine the functional form of the potential, as we know the numerical values of Γ for all relevant values of N. In this case, one will have to solve a second-order differential equation for $V(\phi)$ for each N, as the expression of Γ contains $V_{,\phi\phi}$. This shows that one can, in principle, determine the approximate functional form of the potential in multiple ways.

[3]One can easily find out how this potential evolves with N, as we know how $V(\phi)$ depends on ϕ and $\phi = \phi(N)$.

2. Phantom tachyon ($\epsilon = -1$)

After the normal tachyons, we will now deal with the phantom tachyons. From the first Friedmann equation in Eq. (5), it becomes apparently clear that phase space is not constrained, as

$$0 \leq y^2 \leq \sqrt{1 + x^2}. \tag{46}$$

Since $-\infty < x < \infty$, we have $0 < y < \infty$. As a result of this, we will first like to compactify the phase space. To compactify the phase space, we introduce two variables (X, Y) [54] defined as

$$X = \frac{x}{\sqrt{1 + x^2 + y^2}}, \qquad Y = \frac{y}{\sqrt{1 + x^2 + y^2}}. \tag{47}$$

Using these variables, one can observe that our phase space is constrained, as we get

$$0 \leq Y^2 \leq \frac{1 - X^2}{2 - X^2}, \tag{48}$$

where $-1 \leq X \leq 1$. One can now express Eqs. (40), (6b), and (41) in terms of the new variables X and Y. The expressions of λ and Λ for the present case are given in Appendix C 2. In this case, we have nine critical points of the system which are tabulated in Table V. In order to have real critical points and positive sound speed, ω_0 must be negative and less than ω_1; hence, we shall analyze the system for $\omega_0 = -3$ and $\omega_1 = 1/2$.

We have shown all the critical points of the system in the present case; these critical points include both positive and negative values of Y, although only the critical points with positive values of Y matter. We have shown the full set of critical points to specify the symmetry of the problem. The value of λ for the critical points P_3 to P_6 can be found from the plot in Fig. 6. The plot shows a contour, where in the white region there exists no real, finite value of λ. The color codes give the range of λ values which one may expect if one chooses appropriate (ω_0, ω_1) pairs.

In Table VI, we have represented the critical points for $\omega_0 = -3$ and $\omega_1 = 1/2$ for $\epsilon = -1$. The table shows the values of various parameters of the model for the specific values of ω_0, ω_1, and ϵ. One can see that in this present case one can have superluminal sound propagation. This effect is particular to this model, and one cannot modify this result. In the present case, as $\omega_{\mathrm{tot}} = -c_s^2$ we will always have $c_s^2 > 1$ for the phantom case $\omega_{\mathrm{tot}} < -1$. Lately, it is known that various kinds of k-essence theories can, in principle, have superluminal sound propagation. This propagation happens only in the medium with a specific configuration of scalar fields and not in vacuum. In a certain way, Lorentz invariance is not lost because of the particular medium produced by the scalar field.

TABLE V. The critical points and corresponding physical parameters for $\epsilon = -1$.

Critical points in terms of compact variables						
Points	X	Y	$\omega_{\rm tot}$	c_s^2	Γ	λ
P_0	0	0	0	1	∞	∞
$P_{1,2}$	$\mp\frac{\sqrt{\omega_0+1}}{\sqrt{\omega_0}}$	0	0	$-\omega_0$	$\frac{3+2\omega_0}{2(1+\omega_0)}$	∞
$P_{3,4}$	$-\frac{\sqrt{\sqrt{\omega_1-\omega_0}+\omega_0-\omega_1}}{\sqrt{\omega_0-\omega_1}}$	$\mp\frac{\sqrt{(\omega_0-1)\sqrt{\omega_1-\omega_0}-2\omega_0+\omega_1}}{\sqrt{-(\omega_0-\omega_1+1)(\sqrt{\omega_1-\omega_0}+\omega_0)}}$	$\omega_0-\omega_1$	$-\omega_0+\omega_1$	3/2	See Fig. 6
$P_{5,6}$	$\frac{\sqrt{\sqrt{\omega_1-\omega_0}+\omega_0-\omega_1}}{\sqrt{\omega_0-\omega_1}}$	$\mp\frac{\sqrt{(\omega_0-1)\sqrt{\omega_1-\omega_0}-2\omega_0+\omega_1}}{\sqrt{-(\omega_0-\omega_1+1)(\sqrt{\omega_1-\omega_0}+\omega_0)}}$	$\omega_0-\omega_1$	$-\omega_0+\omega_1$	3/2	See Fig. 6
$P_{7,8}$	0	$\pm 1/\sqrt{2}$	-1	1	∞	0

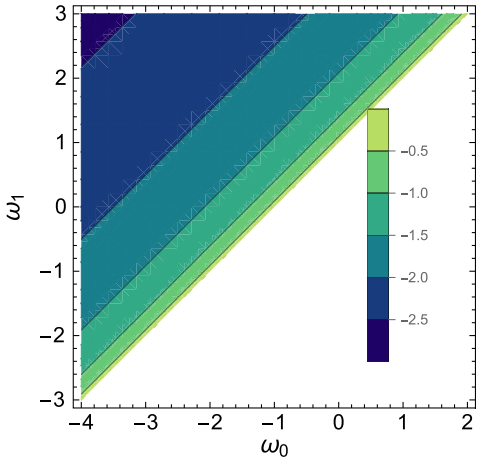

FIG. 6. The values of λ corresponding to the fixed points P_3 to P_6 are ω_0 and ω_1 dependent. Here, λ is negative if both (X, Y) have the same sign and positive for the alternate sign (keeping $|X|, |Y|$ the same), while the magnitude of λ remains the same in both cases.

In the phase space Fig. 7, we have plotted X vs Y. The phase space is constrained, and there exist three separate regions. In this case, $P_{1,2}$ are the nonaccelerating points having an equation of state zero. All the vector fields originating from these points are attracted toward P_4, P_6, and P_8. Although the system near these points shows phantom nature, none of them are stable fixed points except P_8. In this system, only the point P_8 is a stable attractor point, and all the nearby trajectories are attracted toward it; hence, it is a global attractor.

TABLE VI. Critical points for $\omega_0 = -3$ and $\omega_1 = 1/2$.

Points	(X, Y)	$\omega_{\rm tot}$	c_s^2	Stability
P_0	(0, 0)	0	1	Unstable
$P_{1,2}$	$(\mp\sqrt{2/3}, 0)$	0	3	Unstable
$P_{3,4}$	$(-0.68, \mp 0.59)$	$-7/2$	7/2	Saddle
$P_{5,6}$	$(0.68, \mp 0.59)$	$-7/2$	7/2	Saddle
$P_{7,8}$	$(0, \mp 1/\sqrt{2})$	-1	1	Stable

The physical nature of the system can be explained by plotting the dynamical variables against N as shown in Fig. 8. We found numerically that at the late time P_8 is the stable point and the system evolves toward it. The evolution starts from the distant past with an EOS close to zero. This phase resembles the dark-matter-dominated regime. In this era, the fluid energy density dominates phantom tachyon energy density. Sound speed corresponding to this era is greater than one. As the system evolves, the fluid energy density starts decreasing, and the tachyon energy density starts to dominate. As a result of this, the EOS of the system saturates at -1 and sound speed becomes 1. We have also plotted the functions related to the potential: λ and Γ. In the early epoch, λ decreases exponentially, while Γ has a controlled behavior. As the system evolves, both Γ and λ start increasing. In the transition from dark matter to dark energy, phase Γ saturates to a value 1 and λ goes to zero.

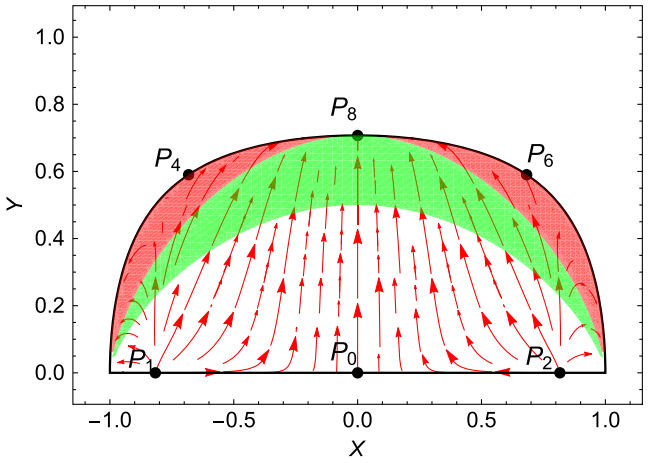

FIG. 7. The phase space plot for $\epsilon = -1$, $\omega_0 = -3$, and $\omega_1 = 1/2$. The phase space is constrained; in the green region we have $-1 \le \omega_{\rm tot} < -1/3$, and in the red region $\omega_{\rm tot} < -1$.

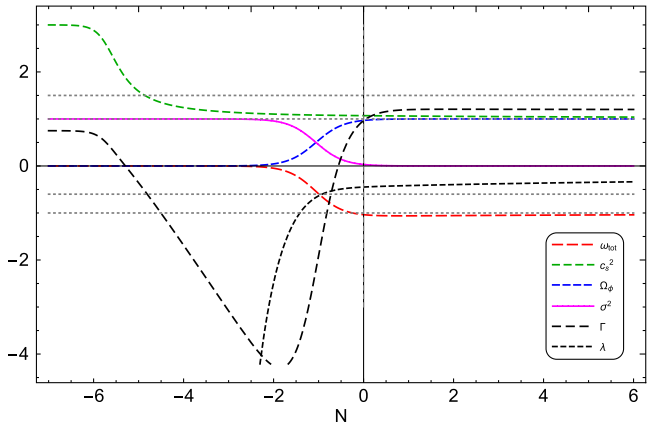

FIG. 8. The evolution plot for $\epsilon = -1$, $\omega_0 = -3$, and $\omega_1 = 1/2$.

IV. INTERACTING TACHYON WITH PRESSURELESS FLUID

In this section, we extend our analysis to the interacting dark sector scenario, i.e., where the tachyon field is coupled with the pressureless matter. Dynamical system analysis of a tachyonic field coupled to matter is usually a complicated exercise. We consider a simple interaction of the form

$$\mathbb{Q} = Q\rho_b\dot{\phi}H, \tag{49}$$

where Q is a dimensionless constant.[4] In our case, the coupled conservation equations become

$$\dot{\rho}_b + 3H\rho_b = \mathbb{Q} = Q\rho_b\dot{\phi}H, \tag{50a}$$

$$\dot{\rho}_\phi + 3H(P_\phi + \rho_\phi) = -\mathbb{Q} = -Q\rho_b\dot{\phi}H. \tag{50b}$$

The coupling term modifies the field equation (2c) as

$$\ddot{\phi} + 3H(1-\epsilon\dot{\phi}^2)\dot{\phi} + \frac{\epsilon V_{,\phi}}{V}(1-\epsilon\dot{\phi}^2) = -\frac{\epsilon Q H\rho_b}{V}\left(1-\epsilon\dot{\phi}^2\right)^{3/2}. \tag{51}$$

From the above equation and using the dimensionless variables in Eq. (4), the dynamical equation for x can be written as

$$x' = -\epsilon Q\frac{\sigma^2}{y^2}(1-\epsilon x^2)^{3/2} + \epsilon\lambda\sqrt{3}y(1-\epsilon x^2) - 3x(1-\epsilon x^2), \tag{52}$$

or, using the constraint equation (5),

$$x' = -\epsilon Q\left(\frac{(1-\epsilon x^2)^{3/2}}{y^2} - (1-\epsilon x^2)\right) + \epsilon\lambda\sqrt{3}y(1-\epsilon x^2) - 3x(1-\epsilon x^2). \tag{53}$$

The dynamical equations of y and λ remain the same.

Note that, in general, a coupling term is expected to give rise to an additional dimensionality in the phase space, requiring us to define an additional dynamical variable. In fact, a generic coupling term may not even allow us to close the system to write it in an autonomous form. Our specific choice of the coupling term in Eq. (49), however, does not require us to define an additional dynamical variable. The dimensionality of the phase space remains the same.

We now proceed to investigate the compatibility of our equation of state parametrizations with the choice of this coupling. We note that the issue with the Taylor series parametrizations that we outlined in Sec. III A 5 is independent of whether there is dark sector coupling or not; this is an inherent issue with the parametrization itself while trying to recast it as a constraint over the phase space. Therefore, in what follows, we will concentrate only on the second parametrization introduced in Sec. III B. Since our goal here is not an extensive analysis of the tachyonic model but to showcase the applicability of the framework we developed, we will concentrate only on the canonical tachyon case ($\epsilon = +1$).

A. Interacting canonical tachyon with the second parametrization

Proceeding in the same way, one can express λ as

$$\lambda(x,y) = \frac{2Q(y^2-\sqrt{1-\epsilon x^2})(x^4+(\omega_0+1)(x^2\epsilon-2))}{4\sqrt{3}y^3(\omega_0+1)(1-x^2\epsilon)} + \frac{3xy^2(x^2\epsilon(2(\omega_0+1)\sqrt{1-x^2\epsilon}+y^2(\omega_0+\omega_1+1))-4(\omega_0+1)\sqrt{1-x^2\epsilon}+x^4(2\sqrt{1-x^2\epsilon}-y^2))}{4\sqrt{3}\epsilon y^3(\omega_0+1)(1-x^2\epsilon)}. \tag{54}$$

[4]This form of coupling is very much similar to Ref. [55], where a coupling term $Q\rho_{de}H$ was shown to reasonably lower the tension between Planck CMB data and DES measurements.

The above expression of $\lambda(x,y)$ has a pole of order three at $y \to 0$. After inserting this in x' or y', one finds that both the equations still have a pole of order two at $y \to 0$. This can be regularized by redefining the time variable as

$$dN \mapsto y^2 dN. \tag{55}$$

With this time redefinition, the new autonomous equation for the canonical tachyon field $\epsilon = +1$ can be written as

$$x' = \frac{\left[\frac{3}{2}\frac{xy^4}{\sqrt{1-x^2}}(-\omega_1 + x^2 - 1 - \omega_0) - \sqrt{3}\lambda(x,y)y^3(x^2 - 1 - \omega_0)\right]}{2 - (x^2 - 1 - \omega_0)(2/x^2 + 1/(1-x^2))}, \tag{56a}$$

$$y' = \frac{y}{2}\left[-\sqrt{3}\lambda(x,y)xy^3 - 3\sqrt{1-x^2}y^4 + 3y^2\right], \tag{56b}$$

which is now completely regular at $y \to 0$ because of the existence of the $\lambda(x,y)y^3$ term in both the equations. The 2D autonomous system presents two invariant submanifolds $x = 0$ and $y = 0$ [noting that $\lambda(0,y) = 0$]. Finding the critical points of this system in all generality is challenging, since the interaction term greatly complicates the system, as clear from the expression of $\lambda(x,y)$ in Eq. (54). The generic critical point structure of the system will depend on three parameters (ω_0, ω_1, Q). Changes to these variables can have far-reaching effects on the dynamics.

Nonetheless, we find that there exist critical points P_0, P_1, and P_2 corresponding to decelerated matter-dominated phases of expansion ($\omega_{\rm tot} = 0$) and fixed points $P_{7,8}$ corresponding to accelerated de Sitter phases of expansion ($\omega_{\rm tot} = -1$); see Table VII. These are the same points that appeared in Table III, i.e., for the noninteracting canonical tachyon case. Therefore, the introduction of an interaction term, at least in the form of Eq. (3), does not affect these critical points. The interaction term destroys the other critical points from the noninteracting scenario while introducing possible others.

As stated, there can be many other critical points depending on the parameter values (ω_0, ω_1, Q), and it is hard to investigate the critical point structure in all generality. However, what our framework does allow is to find the value of the unspecified model parameter Q in terms of the model parameters (ω_0, ω_1), whose value we can get from the observations, for a particular cosmological solution to exist. We explain the procedure below. Let us try to look for critical points (x_*, y_*) whose coordinates satisfy the relation

$$y_*^2\sqrt{1-x_*^2} = -h, \tag{57}$$

h being a constant. Such fixed points lie on the curve $y^2\sqrt{1-x^2} + h = 0$ in the x-y plane, which is the locus of all the points in the phase space whose cosmology is specified by an equation of state parameter $\omega_{\rm tot} = h$. Next, we adopt the following strategy. We utilize the condition (57) to replace the combination $y^2\sqrt{1-x^2}$ whenever it arises in Eqs. (56a) and (56b). This reduces the complexity of the expressions significantly. Next, we solve algebraically for the critical points from these simplified equations. We will find the coordinates of the critical points in terms of $(h, \omega_0, \omega_1, Q)$. However, for consistency, we must substitute these coordinates back in Eq. (57). This gives us a condition on the model parameters (ω_0, ω_1, Q).[5] Only when the model parameters satisfy this particular consistency condition can a critical point satisfying the condition (57) exist. In our framework, we use the numerical values of (ω_0, ω_1) obtained from the observations, whereas Q is still unspecified. Therefore, with this approach, given a pair of values for (ω_0, ω_1) one can determine the value of Q such that there exists a critical point whose cosmology is specified by $\omega_{\rm tot} = h$. In particular, it is worthwhile to check that, for a given (ω_0, ω_1), for what values of Q our interaction term in Eq. (49) can allow for the existence of other possible matter-dominated phases ($h = 0$) and other possible accelerated phases ($-1 \le h < -1/3$).

Following the above strategy, we find another critical point P_3 (see Table VII). We remind the reader that this critical point P_3 is *not* the same P_3 that appeared in Table III. The consistency condition between the model parameters for the existence critical point P_3 is obtained by putting its coordinates back in Eq. (57), and it can be expressed as

$$(2+h)\left(\frac{9h^2}{Q^2}\right)^2 + [(1+\omega_0+\omega_1)h - 2(1+h)(2+\omega_0)]\left(\frac{9h^2}{Q^2}\right) + 2(1+h)(1+\omega_0) = 0. \tag{58}$$

TABLE VII. Second parametrization critical points.

Critical points for $\epsilon = +1$			
Points	x	y	$\omega_{\rm tot}$
P_0	0	0	0
$P_{1,2}$	$\mp\sqrt{1+\omega_0}$	0	0
P_3	$-\frac{3h}{Q}$	$\left[\frac{2Q}{3}\left(\frac{1+h}{-h}\right)\left(\frac{9h^2-Q^2(\omega_0+1)}{9h^2-Q^2(\omega_0+\omega_1+1)}\right)\right]^{1/4}$	h
$P_{7,8}$	0	∓ 1	0

[5] An alternative way to get this condition is to replace y_*^2 by $-\frac{h}{\sqrt{1-x_*^2}}$, solve the equation $x'|_{x_*} = 0$ to obtain $x_* = x_*(\omega_0, \omega_1, Q)$, and then put $x_* = x_*(\omega_0, \omega_1, Q)$, $y_*^2 = -\frac{h}{\sqrt{1-x_*^2}}$ in the equation $y'|_{(x_*, y_*)} = 0$.

Within the observationally allowed range of model parameters, $1+\omega_0 > 0$. Also, let us confine ourselves to the case when the critical point P_3 is not phantom, i.e., $h > -1$. Then, two real positive roots for $9h^2/Q^2$ exist when the following condition is met:

$$(1+\omega_0+\omega_1)h - 2(1+h)(2+\omega_0) \leq -\sqrt{8(1+h)(2+h)(1+\omega_0)}. \tag{59}$$

Henceforth, we focus on the case $Q > 0$; one can follow similar steps for $Q < 0$. Provided that the condition (59) is satisfied, for any given ω_0 and ω_1, one gets two possible values of Q so that the critical point P_3 can exist:

$$Q_{\mp} = \frac{3}{2\sqrt{(h+1)(\omega_0+1)}}\Big[(h^3(\omega_0-\omega_1+3)+2h^2(\omega_0+2)) \mp \sqrt{h^4(h^2\omega_1^2 - 2h\omega_1((h+2)\omega_0+3h+4)+(h(\omega_0-1)+2\omega_0)^2)}\Big]^{1/2}. \tag{60}$$

Based on Q_- and Q_+, one actually gets two different versions of P_3, which we denote by P_{3-} and P_{3+}, respectively.

In Fig. 9, we show using color pallets the range of values of the interaction parameters Q_- and Q_+, against the model parameters ω_0 and ω_1 such that the critical point P_3 may represent accelerated expansion phases with $\omega_{\rm tot} = h = (-0.8, -0.9)$. We emphasize that the condition (59), which is the condition for having real values of $Q_{\mp}$, by itself is only a *necessary, but not sufficient* condition for

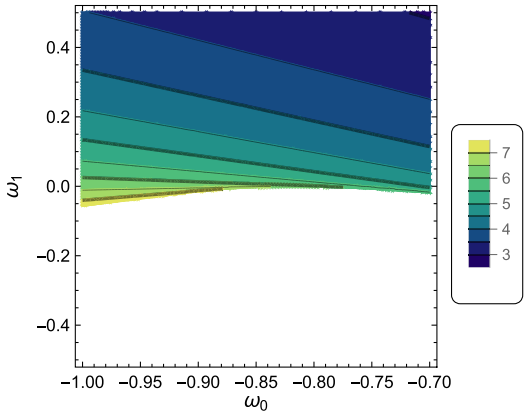

(a) The constraint on Q_- for $h = -0.9$

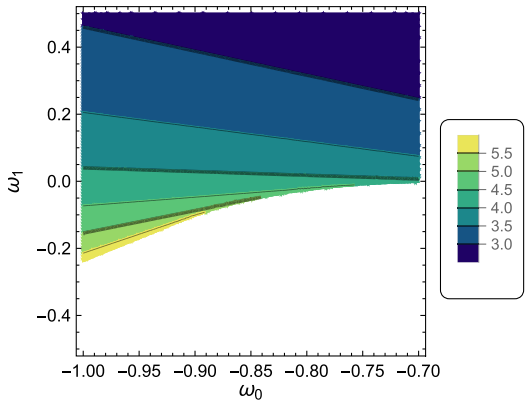

(b) The constraint on Q_- for $h = -0.8$

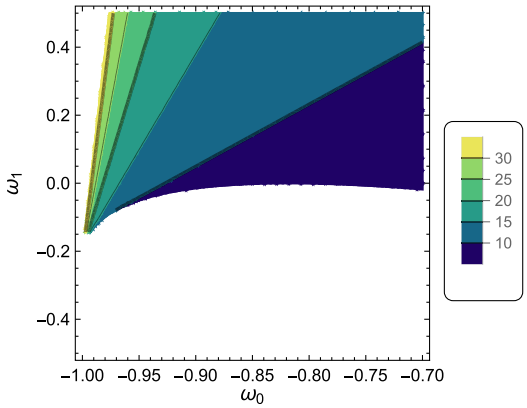

(c) The constraint on Q_+ for $h = -0.9$

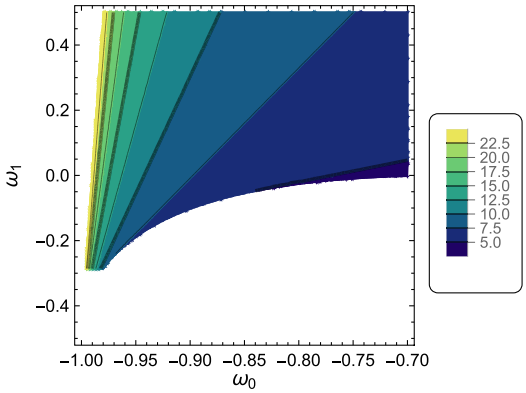

(d) The constraint on Q_+ for $h = -0.8$

FIG. 9. The color pallets show the range of values of the interaction parameters Q_- and Q_+ against the model parameters ω_0 and ω_1 such that the critical point P_3 may represent accelerated expansion phases with $\omega_{\rm tot} = h = (-0.8, -0.9)$. The entire shaded region is the region specified by the constraint (59).

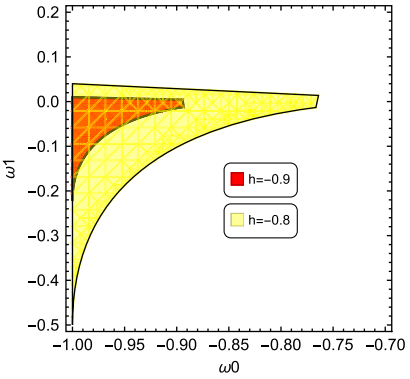

(a) The existence of point P_{3-} for $h = -0.9, -0.8$.

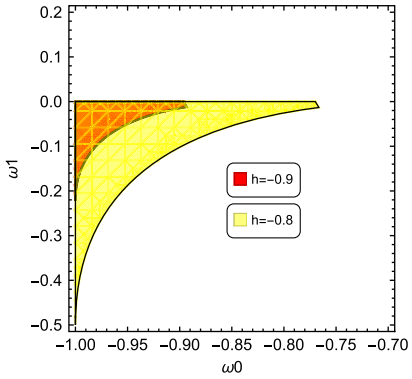

(b) The existence of point P_{3+} for $h = -0.9, -0.8$.

FIG. 10. The range in the parameter space $\omega_0 - \omega_1$ such that the critical points P_{3-} and P_{3+} can exist.

critical points $P_{3\mp}$ to exist. One needs to put the values of $Q_{\mp}$ from Eq. (60) back in the coordinates of P_3 in Table VII and demand that the y coordinate is real. This gives a further constraint on the allowed values of the model parameters (ω_0, ω_1) for critical points $P_{3\mp}$ to exist, which we show in Fig. 10. This is the region in the parameter space (ω_0, ω_1) such that it is possible for the interaction model of Eq. (49) to support, for some value of the interaction parameter Q, the existence of critical points P_{3-} or P_{3+} with $\omega_{\rm tot} = h$.

The above strategy, of course, does not allow us to find the entire set of critical points. Given the numerical values of the model parameters (ω_0, ω_1, Q), we can find the critical points numerically. As an example, in Table VIII we list the physically viable (i.e., allowed by the Friedmann constraint) critical points numerically obtained for the parameter choice $\omega_0 = -0.9$, $\omega_1 = -0.1$, and $Q = 4$. The corresponding phase space is depicted in Fig. 11, in which the green region shows an accelerating phase and the sound speed is positive and subluminal in the entire region. The points P_0 and P_2 both represent matter-dominated cosmological epochs. However, P_2 is a stable point, so it cannot really represent the actual matter-dominated epoch that our Universe has gone through. On the other hand, P_0 is unstable, and, therefore, it can represent a cosmologically relevant matter-dominated epoch. The three points P_3, P_4, and P_8 represent accelerated cosmological epochs, with P_8 being a de Sitter phase. The saddle fixed point P_4 is a perfectly viable candidate to characterize the present accelerated epoch of the Universe, since the fractional field density is ≈ 0.71 and the fractional fluid density is ≈ 0.29. Figure 11 shows the existence of heteroclinic trajectories connecting the matter-dominated unstable phase P_0 to the stable accelerated phase P_3 through the present intermediate phase P_4, representing a possible viable course of evolution for our Universe. The stable point P_3, which is an accelerated phase dominated completely by the tachyonic field ($\Omega_\phi = 1$), represents the future asymptotic of the cosmological evolution.

We investigated the dynamics of the coupled system depicted in Fig. 12 for some initial conditions. In the early phase, the fluid density outweighs the field density. The total EOS is close to zero, which may mimic the matter phase. In the minimally coupled field-fluid system, the total

TABLE VIII. The critical points for $\omega_0 = -0.9$, $\omega_1 = -0.1$, $Q = 4$, and $\epsilon = +1$ corresponding to the second parametrization.

Critical points for $\epsilon = +1$							
Points	x	y	Ω_ϕ	σ^2	$\omega_{\rm tot}$	c_s^2	Stability
P_0	0	0	0	1	0	1	Unstable
P_2	0.32	0	0	1	0	0.90	Stable
P_3	0.45	0.95	1	0	−0.80	0.80	Stable
P_4	0.32	0.68	0.71	0.52	−0.43	0.89	Saddle
P_8	0	1	1	0	−1	1	Saddle

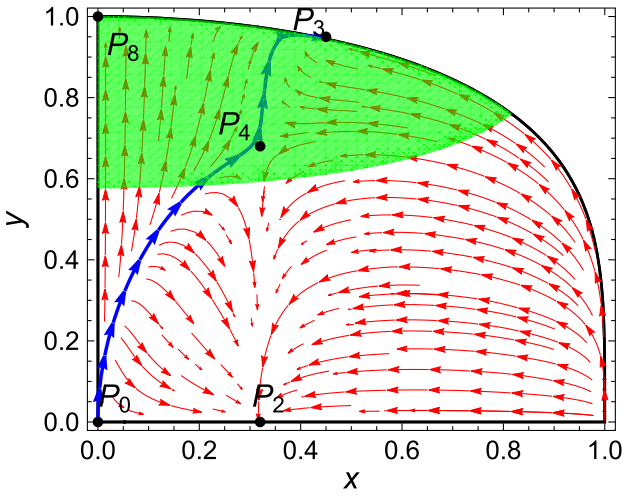

FIG. 11. The phase space of the coupled system for $\omega_0 = -0.9$, $\omega_1 = -0.1$, $Q = 4$, and $\epsilon = +1$ corresponds to the second parametrization.

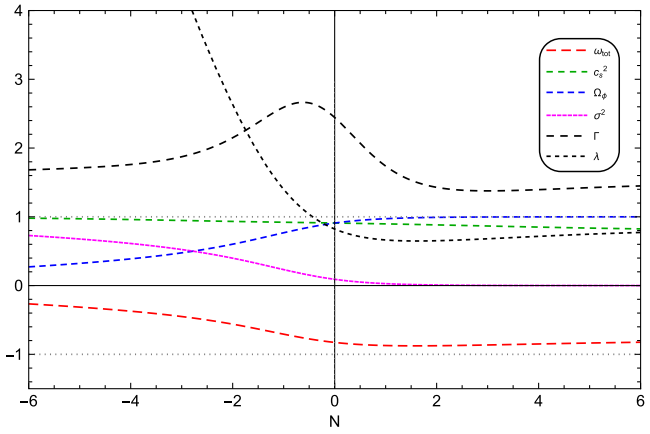

FIG. 12. The evolution of the coupled system for $\omega_0 = -0.9$, $\omega_1 = -0.1$, $Q = 4$, and $\epsilon = +1$, corresponding to the second parametrization.

EOS remains zero at this phase; however, in the coupled system, the field density does not dilute to zero. Consequently, the EOS is not zero. In this phase, Γ, sound speed c_s^2, and λ have nonzero values. As the field density grows, Γ demonstrates a rising trend before saturation at some finite value in the late time. Throughout this phase transition, λ has a declining trend and becomes saturated. In the late-time phase, the field density dominates over the fluid density. As a result, the total EOS of the system approaches -0.8. The sound speed remains close to 1.

V. CONCLUSION

In this paper, we have studied the dynamics of tachyon-dark-energy models for both the canonical and phantom scalar field. Tachyon-dark-energy models were studied for more than decades, but here we have studied it from a completely new perspective. In all of the previous studies, the tachyon potential was assumed to be some function of the tachyon field, or the potential parameter Γ was assumed to have some preassigned value. Once this information was known, the dynamics and EOS of the evolving system was calculated. In the present paper, we have not assumed any prior form of the tachyon potential; rather, we have considered parametrization of the EOS of the scalar field. Our work is motivated by various approximate forms of the EOS of the tachyon field.

It is seen that once we introduce an approximate EOS for the tachyon field the autonomous equations guiding the system changes its form. One of the dynamical variables of the system, namely, λ, becomes redundant, as we do not require one to explicitly solve for λ to predict the dynamics of the system. Consideration of the parametrization of EOS of the scalar field reduces the phase space dimension of the system by one, and, ultimately, a 3D system reduces to a 2D one. This dimensional reduction of the system, on the other hand, gives a functional form of Γ which, in general, can include a large class of potentials. We studied important dynamical characteristics of the evolving system using our prescription together with the evolution of the important cosmological parameters. The method applied is self-consistent, and, consequently, we can smoothly use the phenomenologically motivated approximate EOS of the tachyon field. Our method is fairly general, and we expect that this method can be applied in other dynamic dark energy models.

To show the effectiveness of our proposal, we have used two kinds of parametrization to write the EOS of the tachyon field. The first parametrization is more like a Taylor series expansion of the EOS around the present time. In this Taylor series, we retain only the first two terms and use it to solve the dynamical system. In solving the autonomous equations, in some of the cases, we had to redefine time and use compactified variables to figure out the critical points of the system. The cosmological dynamics of corresponding to this parametrization shows certain limitations. It is seen that one of the phase space variables, $x(N)$, is either defined only in the future or defined only in the past. This property, of the Taylor series parametrization, is a serious limitation of this particular form of the approximate EOS.

To obtain a viable cosmology, we have used another form of parametrization of the EOS of the tachyon field. In the second parametrization, the EOS of the tachyon field is expressed as a sum of a constant term and a time-dependent part. The EOS closely resembles the dark energy EOS when the Hubble parameter tends to be a constant. We have presented the solutions in a detailed manner, showing the dynamical evolution of various cosmological variables. In the case of phantom tachyons, it is seen that the sound speed in the scalar field sector persistently remains superluminal. We have also verified that superluminal sound propagation in this case cannot be avoided. This kind of behavior arises in some k-essence models of dark energy. In principle, this superluminal speed does not break Lorentz invariance, as this speed is appropriately observed only in a particular tachyonic background.

Although a particular form of the potential of the tachyon field was not assumed *a priori* nor have we assumed any particular functional form of Γ to start with, we have described an approximate method using which one can figure out the form of the tachyon potential $V(\phi)$. The method is approximate, because the form of the potential may not match the exact potential form at all cosmological phases. In the example, we have shown two approximate forms of the potential which matches with the desired exact potential in the late phase of cosmic evolution. In principle, one can use more accurate techniques to find out the functional form of the potential, but, as the potential does not play any primary role in our analysis, we have not attempted to do so.

The applicability of our approach is not confined to noninteracting scenarios only. We have shown it explicitly by considering a simple example of tachyon and dark matter interaction. In general, the interaction terms call for the introduction of an additional dynamical variable, increasing the dimensionality of the phase space. However, for the specific model we considered here (49), namely, $\mathbb{Q} = Q\rho_b\dot{\phi}H$, we did not have to introduce an additional dynamical variable. The dimensionality of the phase space remains the same. Given the numerical values of the model parameters (ω_0, ω_1), our framework allows us to determine the interaction parameter Q so that the interacting model given by Eq. (49) can support the existence of specific cosmological epochs. For given numerical values of the parameters (ω_0, ω_1, Q), one can analyze the dynamics of the phase space without explicitly specifying the potential of the tachyon field. In principle, our framework can also be extended to incorporate more complicated interacting models.

In summary, we have presented a new perspective to the dynamical system analysis of a tachyon-dark-energy model. Our approach is generic and can be applied to other scalar field dark energy models.

ACKNOWLEDGMENTS

S. C. acknowledges funding support from the NSRF via the Program Management Unit for Human Resources and Institutional Development, Research and Innovation [Grant No. B01F650006].

APPENDIX A: CALCULATION OF Γ FOR THE FIRST PARAMETRIZATION

Taking the derivative of the above equation with respect to the N and using Eq. (6c), we will get Γ in terms of x and y as

$$\Gamma = \frac{1}{\epsilon(-6x^5\epsilon^2 + 6x^3\epsilon + x\omega_1)^2}\left[36x^{10}\epsilon^5 - 18x^8\epsilon^4\left(y^2\sqrt{1-x^2\epsilon} + 3\right) + 18x^6\epsilon^3\left(2y^2\sqrt{1-x^2\epsilon} - \omega_1\right)\right.$$
$$\left. - x^2\omega_1\epsilon\left(3y^2\sqrt{1-x^2\epsilon} + 2\omega_1 + 3\right) + 3x^4\epsilon^2\left(y^2(\omega_1 - 6)\sqrt{1-x^2\epsilon} + 7\omega_1 + 6\right) + \omega_1^2\right]. \tag{A1}$$

For the phantom case after the compactification the Γ can be expressed as

$$\Gamma = \frac{1}{(Y^2-1)(X^5\omega_1 - 2X^3(\omega_1+3) + X\omega_1)^2}\left[-18X^4\sqrt{1-X^2}Y^2 + 18X^4(3X^2-1)(Y^2-1)\right.$$
$$+ 3X^2\sqrt{1-X^2}Y^2\omega_1 - 6X^4\sqrt{1-X^2}Y^2\omega_1 + 3X^6\sqrt{1-X^2}Y^2\omega_1 - 3(5X^2+1)$$
$$\left.(X-X^3)^2(Y^2-1)\omega_1 - (X^2-1)^4(X^2+1)(Y^2-1)\omega_1^2\right]. \tag{A2}$$

From here, we found that $\Gamma = 1$ at critical points $(X, Y) = (1, 0)$ and becomes infinite for the other critical point.

APPENDIX B: STABILITY OF THE FIXED POINTS FOR THE CASE OF PHANTOM TACHYONS IN THE FIRST PARAMETRIZATION

The fixed points listed in Table II are nonhyperbolic. Therefore, their stability cannot be determined via the usual Jacobian analysis. In these situations, one can resort to a more formal center manifold analysis, but we notice that there is a way around here. The trick is to look for invariant submanifolds of the system described by Eq. (27). From Eq. (27), we can directly observe that $X = 1$ and $Y = 0$ are invariant submanifolds of the system, because

$$X'|_{X=1} = 0, \qquad Y'|_{Y=0} = 0. \tag{B1}$$

There is another invariant submanifold of the system which is not so clearly identified from Eq. (27), namely, $\sigma = 0$. To see that this is indeed an invariant submanifold, one can start from the definition of σ in Eq. (4) and take its derivative with respect to $N = \ln(a)$. Using the time redefinition in Eq. (26) and the definition of the compact dynamical variables in Eq. (21) and after some straightforward calculations, we arrive at

$$\sigma' = -\frac{3}{2}\sigma XY^2\frac{\sqrt{1-X^2}}{1-Y^2}, \tag{B2}$$

where the prime is to be understood as $\frac{d}{dN}$. Clearly, $\sigma = 0$ is an invariant submanifold, as

$$\sigma'|_{\sigma=0} = 0. \tag{B3}$$

In fact, one could have already guessed the existence of this invariant submanifold from the physical argument that, if the Universe starts as a vacuum, it remains so. There is no mechanism in classical gravity by which matter can be produced out of vacuum.

At the vicinity of $X = 1$, $X' > 0$ ($X' < 0$) for $\omega_1 < 0$ ($\omega_1 > 0$). Correspondingly, the invariant submanifold $X = 1$ is attracting nearby phase flows toward it for $\omega_1 < 0$ and repelling nearby phase flows away from it for $\omega_1 > 0$. At the vicinity of $Y = 0$, we have, to the leading order,

$$Y' \approx \frac{1}{2} XY\left(3 - \frac{\omega_1}{2}(1 - X^2)^2\right). \tag{B4}$$

In particular, at the vicinity of the fixed point $P_1 \equiv (X, Y) = (1, 0)$, $Y' \approx \frac{3}{2}XY$, which is always positive in the first quadrant. Therefore, in the vicinity of P_1, the invariant submanifold $Y = 0$ is always repelling nearby flows away from it. At the vicinity of $\sigma = 0$, the flow is always toward $\sigma = 0$, since the coefficient of σ on the right-hand side of Eq. (B2) is always negative in the first quadrant. Therefore, the curve given by Eq. (24), which represents $\sigma^2 = 0$, i.e., vacuum cosmologies, is attracting nearby flows.

The fixed point P_1 lies at the intersection of the invariant submanifolds $X = 1$ and $Y = 0$. Therefore, this fixed point is a saddle for $\omega_1 < 0$ and a repeller for $\omega_1 > 0$. The fixed point P_2 lies at the intersection of the invariant submanifolds $X = 1$ and $\sigma = 0$. Therefore, this fixed point is an attractor for $\omega_1 < 0$ and a saddle for $\omega_1 > 0$.

APPENDIX C: CALCULATION OF Γ FOR THE SECOND PARAMETRIZATION

In this appendix, we present the expressions of Γ for the various values of ϵ in the second parametrization of the EOS for the scalar field.

1. Analysis of λ and Γ for normal tachyon ($\epsilon = 1$) case

The expression of Γ in this case is

$$\begin{aligned}\Gamma = {} & \frac{1}{\left(-4\sqrt{1-x^2}x(\omega_0+1)+x^5(2\sqrt{1-x^2}-y^2)+x^3(2\sqrt{1-x^2}(\omega_0+1)+y^2(\omega_0+\omega_1+1))\right)^2} \\ & \times -16x^{12}+4x^{10}\left(-4\sqrt{1-x^2}y^2+y^4+9\right)-8(\omega_0+1)^2\left(\sqrt{1-x^2}y^2-1\right) \\ & +2x^2(\omega_0+1)\left(\sqrt{1-x^2}y^2(13\omega_0+3\omega_1+13)+y^4(-(\omega_0+\omega_1+1)\right)-6(\omega_0+1)) \\ & +x^8\left(4\sqrt{1-x^2}y^2(3\omega_0+3\omega_1+8)+y^4(-(4\omega_0+6\omega_1+9))-4(\omega_0+6)\right) \\ & -x^4\left(2\sqrt{1-x^2}y^2(\omega_0+1)(13\omega_0+5\omega_1+14)+y^4(-(\omega_0^2-2\omega_0(\omega_1-2)-3\omega_1^2-2\omega_1+3))+4\omega_0(\omega_0+1)\right) \\ & +2x^6\left(\sqrt{1-x^2}y^2(6\omega_0^2+\omega_0(4\omega_1+3)-4\omega_1-3)+y^4(\omega_0(\omega_1+2)+\omega_1^2+5\omega_1+2)+4(\omega_0+1)^2\right).\end{aligned} \tag{C1}$$

Therefore, Γ depends solely on the dynamical variables x and y. We have seen that λ diverges at $\omega_0 \to -1$ and $x \to \pm 1$, while Γ becomes finite. Hence, $\Gamma = -1$ for $x \to \pm 1$. The expression of Γ when $\omega_0 \to -1$ is

$$\begin{aligned}\Gamma = {} & \frac{1}{\left(x^3(2\sqrt{1-x^2}-y^2)+xy^2\omega_1\right)^2}\times\left[-16x^8+4x^6\left(-4\sqrt{1-x^2}y^2+y^4+9\right)-3y^4\omega_1^2+2x^2y^2\omega_1\left(y^2(\omega_1+4)-8\sqrt{1-x^2}\right)\right. \\ & \left.+x^4\left(4\sqrt{1-x^2}y^2(3\omega_1+5)+y^4(-(6\omega_1+5))-20\right)\right].\end{aligned} \tag{C2}$$

2. Expression of λ and Γ for the phantom tachyon field

In the transformed variable λ can be written as

$$\begin{aligned}\lambda = {} & \frac{1}{4Y(\omega_0+1)\left(\frac{Y^2-1}{X^2+Y^2-1}\right)^{3/2}(X^2+Y^2-1)^2}\sqrt{3}X\left[X^4\left(\frac{Y^2}{X^2+Y^2-1}+2\sqrt{\frac{Y^2-1}{X^2+Y^2-1}}\right)\right. \\ & \left.-4(\omega_0+1)\sqrt{\frac{Y^2-1}{X^2+Y^2-1}}(X^2+Y^2-1)^2-X^2(-X^2-Y^2+1)\left(2(\omega_0+1)\sqrt{\frac{Y^2-1}{X^2+Y^2-1}}-\frac{Y^2(\omega_0+\omega_1+1)}{X^2+Y^2-1}\right)\right].\end{aligned} \tag{C3}$$

One can write Γ as

$$\Gamma = \left[\left((X^2+Y^2-1)^5\left(8(\omega_0+1)^2\left(-\frac{Y^2\left(\frac{Y^2-1}{X^2+Y^2-1}\right)^{3/2}}{Y^2-1}-1\right)+\frac{16X^{12}}{(X^2+Y^2-1)^6}-\frac{4X^{10}\left(\frac{Y^2\left(\frac{4(Y^2-1)}{\sqrt{\frac{Y^2-1}{X^2+Y^2-1}}}+Y^2\right)}{(X^2+Y^2-1)^2}+9\right)}{(X^2+Y^2-1)^5}\right.\right.\right.$$
$$-\frac{2X^2(\omega_0+1)\left(-\frac{Y^2\left(\frac{Y^2-1}{X^2+Y^2-1}\right)^{3/2}(13\omega_0+3\omega_1+13)}{Y^2-1}-\frac{Y^4(\omega_0+\omega_1+1)}{(X^2+Y^2-1)^2}-6(\omega_0+1)\right)}{X^2+Y^2-1}$$
$$+\frac{X^8\left(\frac{4Y^2\left(\frac{Y^2-1}{X^2+Y^2-1}\right)^{3/2}(3\omega_0+3\omega_1+8)}{Y^2-1}+\frac{Y^4(4\omega_0+6\omega_1+9)}{(X^2+Y^2-1)^2}+4(\omega_0+6)\right)}{(X^2+Y^2-1)^4}$$
$$+\frac{X^4\left(-\frac{2Y^2(\omega_0+1)\left(\frac{Y^2-1}{X^2+Y^2-1}\right)^{3/2}(13\omega_0+5\omega_1+14)}{Y^2-1}-\frac{Y^4(\omega_0^2-2(\omega_0+1)\omega_1+4\omega_0-3\omega_1^2+3)}{(X^2+Y^2-1)^2}+4\omega_0(\omega_0+1)\right)}{(X^2+Y^2-1)^2}$$
$$\left.\left.\left.-\frac{2X^6\left(\frac{Y^2\left(\frac{Y^2-1}{X^2+Y^2-1}\right)^{3/2}(-\omega_0(6\omega_0+4\omega_1+3)+4\omega_1+3)}{Y^2-1}+\frac{Y^4(\omega_0(\omega_1+2)+\omega_1(\omega_1+5)+2)}{(X^2+Y^2-1)^2}+4(\omega_0+1)^2\right)}{(X^2+Y^2-1)^3}\right)\right)\right]$$
$$\times\left[\left(X^5\left(-\frac{Y^2}{X^2+Y^2-1}-2\sqrt{\frac{Y^2-1}{X^2+Y^2-1}}\right)+4X(\omega_0+1)\sqrt{\frac{Y^2-1}{X^2+Y^2-1}}(X^2+Y^2-1)^2\right.\right.$$
$$\left.\left.+X^3(-X^2-Y^2+1)\left(2(\omega_0+1)\sqrt{\frac{Y^2-1}{X^2+Y^2-1}}-\frac{Y^2(\omega_0+\omega_1+1)}{X^2+Y^2-1}\right)\right)^2\right]^{-1}. \tag{C4}$$

[1] Adam G. Riess *et al.*, Observational evidence from supernovae for an accelerating universe and a cosmological constant, Astron. J. **116**, 1009 (1998).

[2] S. Perlmutter *et al.*, Measurements of Ω and Λ from 42 high redshift supernovae, Astrophys. J. **517**, 565 (1999).

[3] Attila Meszaros, On the reality of the accelerating universe, Astrophys. J. **580**, 12 (2002).

[4] M. Arnaud *et al.*, Planck intermediate results. XXXI. Microwave survey of Galactic supernova remnants, Astron. Astrophys. **586**, A134 (2016).

[5] Christopher P. Ahn, Rachael Alexandroff, Carlos Allende Prieto, Scott F. Anderson, Timothy Anderton, Brett H. Andrews, Éric Aubourg, Stephen Bailey, Eduardo Balbinot, Rory Barnes *et al.*, The ninth data release of the sloan digital sky survey: First spectroscopic data from the SDSS-III baryon oscillation spectroscopic survey, Astrophys. J. Suppl. Ser. **203**, 21 (2012).

[6] T. Padmanabhan, Dark energy: Mystery of the millennium, in *AIP Conference Proceedings* (American Institute of Physics, Melville, NY, 2006), Vol. 861, pp. 179–196.

[7] N. Aghanim *et al.*, Planck 2018 results. VI. Cosmological parameters, Astron. Astrophys. **641**, A6 (2020); **652**, C4(E) (2021).

[8] Shadab Alam, Metin Ata, Stephen Bailey, Florian Beutler, Dmitry Bizyaev, Jonathan A. Blazek, Adam S. Bolton, Joel R. Brownstein, Angela Burden, Chia-Hsun Chuang *et al.*, The clustering of galaxies in the completed SDSS-III baryon oscillation spectroscopic survey: Cosmological analysis of

the DR12 galaxy sample, Mon. Not. R. Astron. Soc. **470**, 2617 (2017).

[9] Florian Beutler, Chris Blake, Matthew Colless, D. Heath Jones, Lister Staveley-Smith, Lachlan Campbell, Quentin Parker, Will Saunders, and Fred Watson, The 6df galaxy survey: Baryon acoustic oscillations and the local Hubble constant, Mon. Not. R. Astron. Soc. **416**, 3017 (2011).

[10] Shadab Alam, Marie Aubert, Santiago Avila, Christophe Balland, Julian E. Bautista, Matthew A. Bershady, Dmitry Bizyaev, Michael R. Blanton, Adam S. Bolton, Jo Bovy *et al.*, Completed SDSS-IV extended baryon oscillation spectroscopic survey: Cosmological implications from two decades of spectroscopic surveys at the Apache Point Observatory, Phys. Rev. D **103**, 083533 (2021).

[11] M. A. Troxel, N. MacCrann, J. Zuntz, T. F. Eifler, E. Krause, S. Dodelson, D. Gruen, J. Blazek, O. Friedrich, S. Samurof *et al.*, Dark energy survey year 1 results: Cosmological constraints from cosmic shear, Phys. Rev. D **98**, 043528 (2018).

[12] T. M. C. Abbott, F. B. Abdalla, A. Alarcon, J. Aleksić, S. Allam, S. Allen, A. Amara, J. Annis, J. Asorey, S. Avila *et al.*, Dark energy survey year 1 results: Cosmological constraints from galaxy clustering and weak lensing, Phys. Rev. D **98**, 043526 (2018).

[13] Elisabeth Krause, T. F. Eifler, J. Zuntz, O. Friedrich, M. A. Troxel, S. Dodelson, J. Blazek, L. F. Secco, N. MacCrann, E. Baxter *et al.*, Dark energy survey year 1 results: Multi-probe methodology and simulated likelihood analyses, arXiv:1706.09359.

[14] Adam G. Riess, Stefano Casertano, Wenlong Yuan, Lucas M. Macri, and Dan Scolnic, Large magellanic cloud cepheid standards provide a 1% foundation for the determination of the hubble constant and stronger evidence for physics beyond ΛCDM, Astrophys. J. **876**, 85 (2019).

[15] Kenneth C. Wong, Sherry H. Suyu, Geoff C.-F. Chen, Cristian E. Rusu, Martin Millon, Dominique Sluse, Vivien Bonvin, Christopher D. Fassnacht, Stefan Taubenberger, Matthew W. Auger *et al.*, H0licow—XIII. A 2.4 per cent measurement of H_0 from lensed quasars: 5.3σ tension between early- and late-universe probes, Mon. Not. R. Astron. Soc. **498**, 1420 (2019).

[16] Sunny Vagnozzi, New physics in light of the H_0 tension: An alternative view, Phys. Rev. D **102**, 023518 (2020).

[17] Sunny Vagnozzi, Fabio Pacucci, and Abraham Loeb, Implications for the Hubble tension from the ages of the oldest astrophysical objects, J. High Energy Astrophys. **36**, 27 (2022).

[18] Eoin Ó. Colgáin, M. M. Sheikh-Jabbari, Rance Solomon, Giada Bargiacchi, Salvatore Capozziello, Maria Giovanna Dainotti, and Dejan Stojkovic, Revealing intrinsic flat ΛCDM biases with standardizable candles, Phys. Rev. D **106**, L041301 (2022).

[19] Pavan Kumar Aluri *et al.*, Is the observable universe consistent with the cosmological principle?, arXiv:2207.05765.

[20] Varun Sahni and Alexei Starobinsky, Reconstructing dark energy, Int. J. Mod. Phys. D **15**, 2105 (2006).

[21] Kazuharu Bamba, Salvatore Capozziello, Shin'ichi Nojiri, and Sergei D. Odintsov, Dark energy cosmology: The equivalent description via different theoretical models and cosmography tests, Astrophys. Space Sci. **342**, 155 (2012).

[22] Christian Armendariz-Picon, V. Mukhanov, and Paul J. Steinhardt, Essentials of k-essence, Phys. Rev. D **63**, 103510 (2001).

[23] Robert R. Caldwell, A phantom menace? Cosmological consequences of a dark energy component with super-negative equation of state, Phys. Lett. B **545**, 23 (2002).

[24] Sean M. Carroll, Mark Hoffman, and Mark Trodden, Can the dark energy equation-of-state parameter w be less than–1?, Phys. Rev. D **68**, 023509 (2003).

[25] Alexander Kamenshchik, Ugo Moschella, and Vincent Pasquier, An alternative to quintessence, Phys. Lett. B **511**, 265 (2001).

[26] Ashoke Sen, Tachyon matter, J. High Energy Phys. 07 (2002) 065.

[27] T. Padmanabhan, Accelerated expansion of the universe driven by tachyonic matter, Phys. Rev. D **66**, 021301 (2002).

[28] Edmund J. Copeland, Mohammad Sami, and Shinji Tsujikawa, Dynamics of dark energy, Int. J. Mod. Phys. D **15**, 1753 (2006).

[29] Luca Amendola and Shinji Tsujikawa, *Dark Energy: Theory and Observations* (Cambridge University Press, Cambridge, England, 2010).

[30] Christian Armendariz-Picon, V. Mukhanov, and Paul J. Steinhardt, Dynamical Solution to the Problem of a Small Cosmological Constant and Late-Time Cosmic Acceleration, Phys. Rev. Lett. **85**, 4438 (2000).

[31] G. W. Gibbons, Cosmological evolution of the rolling tachyon, Phys. Lett. B **537**, 1 (2002).

[32] Luis P. Chimento, Extended tachyon field, chaplygin gas, and solvable k-essence cosmologies, Phys. Rev. D **69**, 123517 (2004).

[33] Anupam Mazumdar, Sudhakar Panda, and Abdel Perez-Lorenzana, Assisted inflation via tachyon condensation, Nucl. Phys. **B614**, 101 (2001).

[34] Ashoke Sen, Field theory of tachyon matter, Mod. Phys. Lett. A **17**, 1797 (2002).

[35] Victor H. Cardenas, Tachyonic quintessential inflation, Phys. Rev. D **73**, 103512 (2006).

[36] Debajyoti Choudhury, Debashis Ghoshal, Dileep P. Jatkar, and Sudhakar Panda, On the cosmological relevance of the tachyon, Phys. Lett. B **544**, 231 (2002).

[37] Muhamad Zahid Mughal and Iftikhar Ahmad, A multi-field tachyon-quintom model of dark energy and fate of the universe, Eur. Phys. J. Plus **136**, 1 (2021).

[38] J. S. Bagla, Harvinder Kaur Jassal, and T. Padmanabhan, Cosmology with tachyon field as dark energy, Phys. Rev. D **67**, 063504 (2003).

[39] Zoltán Keresztes, L. A. Gergely, Vittorio Gorini, Ugo Moschella, and A. Yu Kamenshchik, Tachyon cosmology, supernovae data, and the big brake singularity, Phys. Rev. D **79**, 083504 (2009).

[40] Amna Ali, M. Sami, and A. A. Sen, Transient and late time attractor tachyon dark energy: Can we distinguish it from quintessence?, Phys. Rev. D **79**, 123501 (2009).
[41] Manvendra Pratap Rajvanshi, Avinash Singh, H. K. Jassal, and J. S. Bagla, Tachyonic vs quintessence dark energy: Linear perturbations and CMB data, Classical Quantum Gravity **38**, 195001 (2021).
[42] Nandan Roy and Kazuharu Bamba, Arbitrariness of potentials in interacting quintessence models, Phys. Rev. D **99**, 123520 (2019).
[43] Nandan Roy, Alma X. Gonzalez-Morales, and L. Arturo Urena-Lopez, New general parametrization of quintessence fields and its observational constraints, Phys. Rev. D **98**, 063530 (2018).
[44] Burin Gumjudpai, Tapan Naskar, M. Sami, and Shinji Tsujikawa, Coupled dark energy: Towards a general description of the dynamics, J. Cosmol. Astropart. Phys. 06 (2005) 007.
[45] Edmund J. Copeland, Mohammad R. Garousi, M. Sami, and Shinji Tsujikawa, What is needed of a tachyon if it is to be the dark energy?, Phys. Rev. D **71**, 043003 (2005).
[46] Ricardo C. G. Landim, Coupled tachyonic dark energy: A dynamical analysis, Int. J. Mod. Phys. D **24**, 1550085 (2015).
[47] Qin Fei, Yungui Gong, Jiong Lin, and Zhu Yi, The reconstruction of tachyon inflationary potentials, J. Cosmol. Astropart. Phys. 08 (2017) 018.
[48] Archana Sangwan, Ankan Mukherjee, and H. K. Jassal, Reconstructing the dark energy potential, J. Cosmol. Astropart. Phys. 01 (2018) 018.
[49] J. Wainwright and G. F. R. Ellis, *Dynamical Systems in Cosmology* (Cambridge University Press, Cambridge, England, 1997).
[50] A. A. Coley, *Dynamical Systems and Cosmology* (Kluwer, Dordrecht, Netherlands, 2003).
[51] Mariam Bouhmadi-López, João Marto, João Morais, and César M. Silva, Cosmic infinity: A dynamical system approach, J. Cosmol. Astropart. Phys. 03 (2017) 042.
[52] A. A. Usmani, Partha Pratim Ghosh, Utpal Mukhopadhyay, P. C. Ray, and Saibal Ray, The dark energy equation of state, Mon. Not. R. Astron. Soc. **386**, L92 (2008).
[53] Michel Chevallier and David Polarski, Accelerating universes with scaling dark matter, Int. J. Mod. Phys. D **10**, 213 (2001).
[54] Marcelo Messias, Dynamics at infinity of a cubic chua's system, Int. J. Bifurcation Chaos Appl. Sci. Eng. **21**, 333 (2011).
[55] Eleonora Di Valentino, Alessandro Melchiorri, Olga Mena, and Sunny Vagnozzi, Interacting dark energy in the early 2020s: A promising solution to the H_0 and cosmic shear tensions, Phys. Dark Universe **30**, 100666 (2020).